12 FC.

PARAMETRIC STUDY OF A COMPACT SHEAR FRACTURE SPECIMEN BY FINITE ELEMENT TECHNIQUES

Daniel Hoyniak

Technical Memorandum
File No. TM 76-196
June 14, 1976
Contract No. N00017-73-C-1418

Copy No. 5

The Pennsylvania State University
Institute for Science and Engineering
APPLIED RESEARCH LABORATORY
Post Office Box 30
State College, PA 16801 Univ. Park

NAVY DEPARTMENT

NAVAL SEA SYSTEMS COMMAND

UNCLASSIFIED

SECURITY CLASSIFICATION OF THIS PAGE (When Data Entered)

REPORT DOCUMENTATION PAGE

READ INSTRUCTIONS BEFORE COMPLETING FORM

1. REPORT NUMBER: TM-76-196	2. GOVT ACCESSION NO.
3. RECIPIENT'S CATALOG NUMBER	
4. TITLE (and Subtitle): PARAMETRIC STUDY OF A COMPACT SHEAR FRACTURE SPECIMEN BY FINITE ELEMENT TECHNIQUES.	5. TYPE OF REPORT & PERIOD COVERED: M.S. Thesis, August 1976
	6. PERFORMING ORG. REPORT NUMBER: TM 76-196
7. AUTHOR(s): Daniel Hoyniak	8. CONTRACT OR GRANT NUMBER(s): N0017-73-C-1418
9. PERFORMING ORGANIZATION NAME AND ADDRESS: The Pennsylvania State University, Applied Research Laboratory, P. O. Box 30, ~~State College~~, PA 16801 Univ Park	10. PROGRAM ELEMENT, PROJECT, TASK AREA & WORK UNIT NUMBERS: 97 p.
11. CONTROLLING OFFICE NAME AND ADDRESS: Naval Sea Systems Command, Department of the Navy, Washington, D. C. 20362	12. REPORT DATE: 14 June 1976
	13. NUMBER OF PAGES: 95 pages & figures
14. MONITORING AGENCY NAME & ADDRESS (if different from Controlling Office): Technical memo.	15. SECURITY CLASS. (of this report): Unclassified, Unlimited
	15a. DECLASSIFICATION/DOWNGRADING SCHEDULE

16. DISTRIBUTION STATEMENT (of this Report)

Approved for public release, distribution unlimited, per NSSC (Naval Sea Systems Command), 7/15/76

17. DISTRIBUTION STATEMENT (of the abstract entered in Block 20, if different from Report)

18. SUPPLEMENTARY NOTES

19. KEY WORDS (Continue on reverse side if necessary and identify by block number)

STRAIN ENERGY RELEASE RATE
MOD 2
STRESS INTENSITY FACTOR
FRACTURE SPECIMEN
DISPLACE TECHNIQUE

20. ABSTRACT (Continue on reverse side if necessary and identify by block number)

A compact shear fracture specimen has been proposed for the study of the edge sliding mode, Mode II, of crack propagation. The purpose of this investigation was to numerically determine the effect that crack length, specimen geometry, and applied load, has on the Mode II stress intensity factors for this specimen. Numerical results were compared to those obtained independently by another investigator using boundary collocation and photoelastic techniques. In addition, the initial angle of propagation was numerically determined for

DD FORM 1 JAN 73 1473 EDITION OF 1 NOV 65 IS OBSOLETE

UNCLASSIFIED

SECURITY CLASSIFICATION OF THIS PAGE (When Data Entered)

20. ABSTRACT (continued)

selected specimen configurations and crack lengths. The Mode II stress intensity factors were generated by using displacement and strain energy release rate methods. The initial angle of propagation was obtained by the strain energy density technique.

The optimum specimen configuration established during this investigation has a tang width H = 1.0 inch. This model configuration exhibited a relatively constant nondimensionalized Mode II stress intensity factor for varying crack lengths. For a tang width of 0.5 inch, the nondimensionalized Mode II stress intensity factors were found to be load dependent for short crack lengths. For a tang width H = 1.5 inch, the nondimensionalized Mode II stress intensity factors were influenced by bending of the specimen over the entire range of crack lengths studied. Boundary effects were also noticed, for all specimen configurations studied, as the crack tip approached the upper and lower boundaries of the specimen. The numerically determined initial angle of propagation was found to be 77° for the specimen configurations and crack lengths selected to be investigated. This study also showed the usefulness of the finite element method in determining the Mode II stress intensity factors for different loading conditions and model geometries.

ACKNOWLEDGEMENTS

The author expresses sincere gratitude to Dr. Joseph C. Conway, Associate Professor of Engineering Mechanics, for his encouragement and assistance in the research and preparation of this thesis. Appreciation is also extended to Mr. Hiroshi Honda for his assistance in the programming of the strain energy subroutine, and to the Applied Research Laboratory of The Pennsylvania State University for use of their facilities and support for this research under contract with the Naval Sea Systems Command.

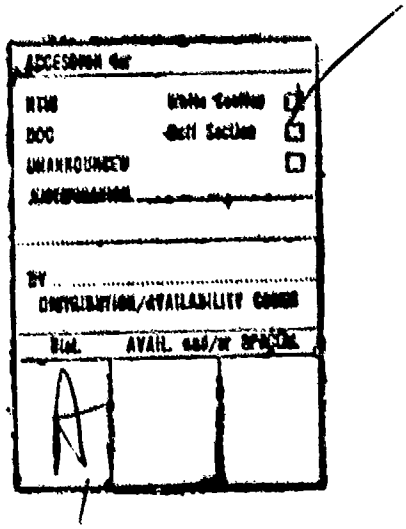

TABLE OF CONTENTS

Page

LIST OF TABLES

LIST OF FIGURES

Figure | Page

CHAPTER I

INTRODUCTION TO PROBLEM

1.1 General Introduction

The use of high-strength materials in the design of engineering structures has lead to the development of theories which can be used to predict the reduced strength of these structures caused by induced or inherent flaws in the material. Engineering fracture mechanics utilizes the concepts of stress intensity factor, K, and critical stress intensity factor, K_c, to predict this reduced strength. The stress intensity factor, K, is a function of applied load and geometry, while the critical stress intensity factor, K_c, is an experimentally determined constant for a given material and mode of deformation.

There are three possible modes of deformation associated with a crack as shown in Figure 1: opening mode, Mode I; edge sliding mode, Mode II; and tearing mode, Mode III. Until recently, Mode I has been considered as the most significant mode of failure. As a consequence, preceding investigations in fracture mechanics have dealt primarily with this mode, and data on critical stress intensity factors is restricted to Mode I loading. Recent investigations, however, indicate that Mode II may be a significant mode of failure in certain cases. Jones and Chisholm [1] established a compact shear fracture specimen to study the phenomenon of Mode II fracture and determine accurate critical stress intensity data.

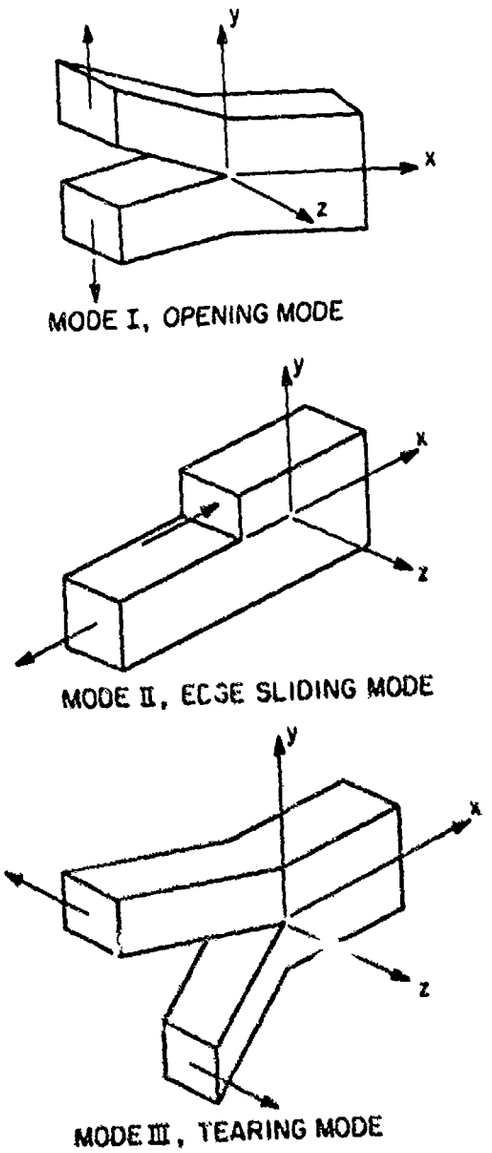

Figure 1. Modes of Crack Deformation

The object of this investigation was to check the performance of the compact shear fracture specimen by numerically generating stress intensity factors using finite element techniques. In addition, initial crack propagation angles were numerically predicted.

1.2 Purpose of Investigation

This study was conducted to investigate, by finite element techniques, the behavior of the compact shear fracture specimen developed by Jones and Chisholm. In particular, Mode II stress intensity factors and stress boundary conditions were numerically generated for comparison with those obtained by Jones using boundary collocation and photoelastic methods. In addition, the initial angle of propagation which could not be obtained by Jones was determined for selected specimen geometry and crack lengths.

1.3 Scope of Investigation

This study utilized the compact shear fracture specimen established by Jones and Chisholm to numerically determine the effect of changing crack length, applied load, and specimen geometry on the Mode II stress intensity factor, K_{II} . The specimen,shown in Figure 2, has a specimen height W , thickness B , crack length a and tang width H . The model parameters varied in this investigation were crack length a , and tang width H .

Point and uniform loads were utilized in this investigation to simulate conditions that could be achieved in a rigid loading frame, and also to approximate as closely as possible the loading conditions adopted by Jones. The stress distribution along the upper boundary and

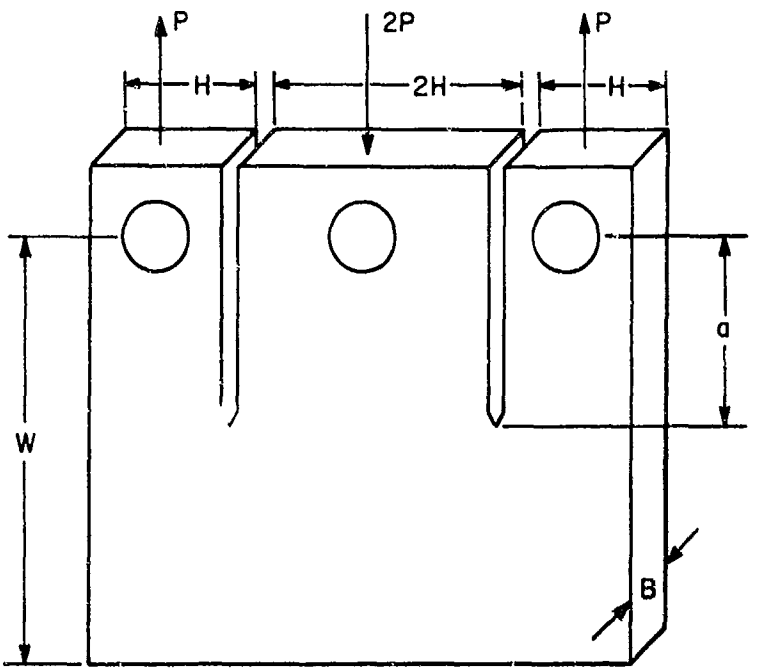

Figure 2. Compact Shear Fracture Specimen

vertical axis of symmetry obtained for selected load conditions and model configurations were compared to those assumed in the boundary collocation study.

The initial angle of propagation of the crack, for a given crack length, applied load, and model geometry, was also determined.

1.4 Approach Used in the Investigation

A numerical solution, the finite element method, was employed to generate displacements along the crack flanks, the normal and tangential stress distribution along the upper tang boundary, and the normal stress distribution along the vertical axis of symmetry. A plane strain condition was utilized for the numerical analysis throughout this investigation.

The stress intensity factors for the various configurations studied were determined by the displacement [2] and strain energy release rate methods [2]. Numerical results were compared to those obtained in a closed form solution for a model with similar configuration and loading conditions, and to the boundary collocation results. A discription of the closed form solution is given in Appendix B.

The numerically generated normal and tangential stresses along the upper boundary and vertical axis of symmetry represented the stress boundary conditions actually occurring in the model for a given load and model configuration. These were compared to the stress boundary conditions assumed by Jones and Chisholm.

A strain energy density technique [6] was used to numerically obtain the initial angle of propagation of the crack for selected crack lengths and specimen geometry.

CHAPTER II

FINITE ELEMENT TECHNIQUES APPLIED TO LINEAR ELASTIC FRACTURE MECHANICS

2.1 Introduction

The finite element method was utilized to generate displacements along the free flanks of the crack, and the normal and tangential stress distributions along the vertical axis of symmetry and upper boundary of the compact shear fracture specimen under consideration. The methods used to calculate Mode II stress intensity factors for given specimen configuration, crack length and applied loading were the displacement method and the method of strain energy release rate. A brief description of the finite element program used is given in Appendix A. The initial angle of propagation for selected cases was numerically determined by the strain energy density method.

2.2 Displacement Method

The displacement method [2] utilized the displacements of nodal points along the crack flanks and equations describing the displacement field near the crack tip. The equations describing the displacement field are those derived by Westergaard [3], and shown below for Mode I and Mode II plane strain deformations. For Mode I loading,

$$u_I = \frac{K_I}{\mu} \left[\frac{r}{2\pi}\right]^{1/2} \cos\frac{\theta}{2} \left[1 - 2\nu + \sin^2\left(\frac{\theta}{2}\right)\right] \qquad (2.1)$$

and

$$v_I = \frac{K_I}{\mu}\left[\frac{r}{2\pi}\right]^{1/2} \sin\frac{\theta}{2}\left[2 - 2\nu - \cos^2\left(\frac{\theta}{2}\right)\right], \qquad (2.2)$$

while for Mode II loading,

$$u_{II} = \frac{K_{II}}{\mu}\left[\frac{r}{2\pi}\right]^{1/2} \sin\frac{\theta}{2}\left[2 - 2\nu + \cos^2\left(\frac{\theta}{2}\right)\right] \qquad (2.3)$$

and

$$v_{II} = \frac{K_{II}}{\mu}\left[\frac{r}{2\pi}\right]^{1/2} \cos\frac{\theta}{2}\left[-1 + 2\nu + \sin^2\left(\frac{\theta}{2}\right)\right], \qquad (2.4)$$

where μ is the shear modulus, ν is Poisson's ratio, r, θ, u and v are defined in Figure 3. K_I and K_{II} are the Mode I and Mode II stress intensity factors.

By using nodal displacements, u^* and v^*, along the crack flank as determined by the finite element method, a stress intensity factor K_I^* or K_{II}^* can be found at each nodal point by use of Equations (2.1) through (2.4). Chan [2] found that the most accurate values of K_I^* and K_{II}^* are attained by using the equations for v_I and u_{II} with $\theta = 180°$. Thus,

$$K_I^* = \left[\frac{(2\pi)^{1/2}E}{4(1-\nu^2)}\right]\frac{v_I^*}{r^{1/2}} \qquad (2.5)$$

and

$$K_{II}^* = \left[\frac{(2\pi)^{1/2}E}{4(1-\nu^2)}\right]\frac{u_{II}^*}{r^{1/2}}. \qquad (2.6)$$

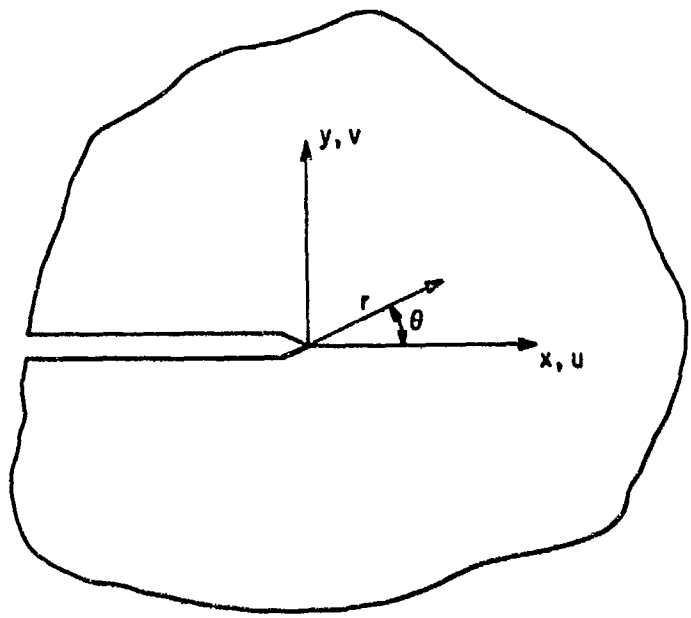

Figure 3. Crack Tip Coordinate System

If the exact displacements were used as r approaches zero, the exact stress intensity will be determined. Since the finite element method gives accurate solutions along the flanks, and very inaccurate solutions at the crack tip, a tangent extrapolation must be used to determine stress intensity factors.

This is accomplished by plotting a graph of the stress intensity factor, K^*, versus the nondimensionalized distance from the crack tip, r/a, Figure 4, using Equations (2.5) and (2.6). A tangent to the straight line region of this curve is then extrapolated back to the point where it intersects the stress intensity axis. This intercept is taken as the value of the stress intensity factor K. A least squares fit to the data in the straight line region was used to determine the intercept in this study. As can be seen in Figure 4, the straight line region does not extend the length of the crack flank. The observed nonlinearity is due to the boundary condition imposed at the load points, and the fact that the equations for displacement, Equations (2.1) through (2.4), are strictly valid near the crack tip. The procedure used in this investigation was to perform a least squares fit in the region of r/a ratios ranging from 0.1 to 0.2.

2.3 Strain Energy Release Rate

The concept of strain energy release rate [2] states that whenever the strain energy released by the structure is greater than the energy needed to create new crack surface area, the crack will propagate unstably. Mathematically, strain energy released rate, G, can be written as:

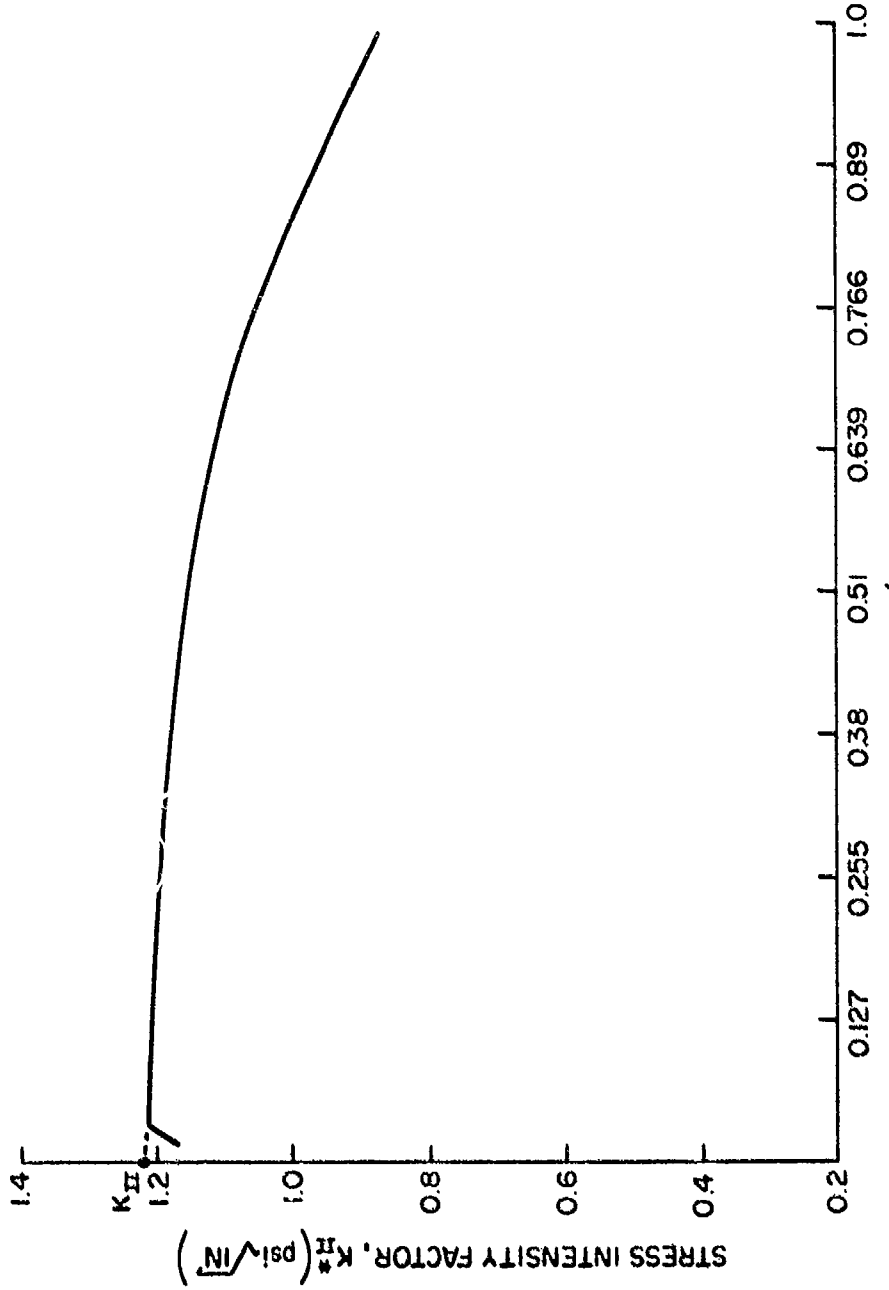

Figure 4. Mode II Stress Intensity Factor Versus r/a for a/W = 0.5, H = 1.0 Inch and a Point Load of P = 1.0 Pound

$$G = \frac{dU}{dA} \quad , \tag{2.7}$$

where U is the strain energy stored in the structure and A is the new crack surface area formed as the crack extends. Strain energy release rate is related to Mode I and Mode II stress intensity factors by the relation [4]

$$K_I^2 + K_{II}^2 = \frac{EG}{1 - \nu^2} \quad . \tag{2.8}$$

This equation is valid for plane strain conditions.

The finite element method can be used to solve for the strain energy release rate, expressed by Equation (2.7), by the following means. The total strain energy of the structure, U_T , is determined by numerically summing the strain energy of each element of the structure. The crack is then extended by a small incremental length, Δa , and the total strain energy, U_T' , is again determined. For plane strain analysis, with the thickness of the model set equal to unity, Equation (2.7) can now be rewritten as:

$$G = \frac{U_T' - U_T}{\Delta a} \quad . \tag{2.9}$$

Utilizing Equation (2.9) and the fact that for the fracture specimen being studied, Mode I stress intensity factors were negative and therefore could be neglected, K_{II} can be determined from the relation:

$$K_I^2 + K_{II}^2 = \frac{E}{1 - \nu^2} \left[\frac{U_T' - U_T}{\Delta a} \right] \quad . \tag{2.10}$$

2.4 Strain Energy Density

Because cracks which are not oriented perpendicular to the applied load tend to propagate in a direction other than along the axis of the crack, Sih [5] proposed the concept of strain energy density in order to analytically determine the direction of crack growth. Sih determined that the magnitude of the energy field in the vicinity of the crack tip can be written as:

$$S = a_{11}K_I^2 + a_{12}K_IK_{II} + a_{22}K_{II}^2 \tag{2.11}$$

where

$$a_{11} = \frac{1}{16\mu}[(1 + \cos\theta)(\kappa - \cos\theta)] \ ,$$

$$a_{12} = \frac{1}{16\mu}\sin\theta[2\cos\theta - (\kappa - 1)]$$

and

$$a_{22} = \frac{1}{16\mu}[(\kappa + 1)(1 - \cos\theta) + (1 + \cos\theta)(3\cos\theta - 1)] \ . \tag{2.12}$$

In these equations, $\kappa = 3 - 4\nu$ for plane strain and $(3 - \nu)(1 + \nu)$ for plane stress problems, θ is defined in Figure 3, μ is the shear modulus and K_I and K_{II} are the Mode I and Mode II stress intensity factors. The concept of strain energy density states that a crack will propagate in the direction for which the strain energy density S possesses a stationary minimum value, or

$$\frac{\partial S}{\partial \theta} = 0 \quad . \tag{2.13}$$

The initial direction of propagation can now be determined by first using finite element techniques to solve for the stress intensity factors, K_I and K_{II}. Equations (2.11) and (2.12) are then used to numerically identify the value of θ which will result in a minimum value of S. In this study, the solution of this problem produced two values of θ which yielded a minimum value of S with the correct value being determined by a physical argument.

CHAPTER III

MODEL USED IN THE INVESTIGATION AND VERIFICATION OF NUMERICAL PROCEDURE

3.1 Introduction

As stated earlier, the model considered in this study is a fracture specimen proposed by Jones and Chisholm and previously shown in Figure 2. This model was gridded for generation of displacements and stresses by the finite element method. The boundary and load conditions applied to the model are discussed in the following paragraphs and verification of the gridding program and finite element technique is established.

3.2 Grid Pattern

A typical grid pattern utilized in this investigation is shown in Figure 5. The pattern consists of a fine region at the crack tip, a transition region and a course region. In the fine region, a typical ratio of element area to the square of crack length, A/a^2, is 2.6×10^{-3} for $a/W = 0.5$. This ratio for the course region is 1.04×10^{-2}. Ratios were chosen in each region to assure optimal convergence to the true solution [2]. The material above the loading pins was not included in the finite element model because it did not contribute any significant stiffness. The fine grid region was moved with the crack tip as crack length was varied. This required that the

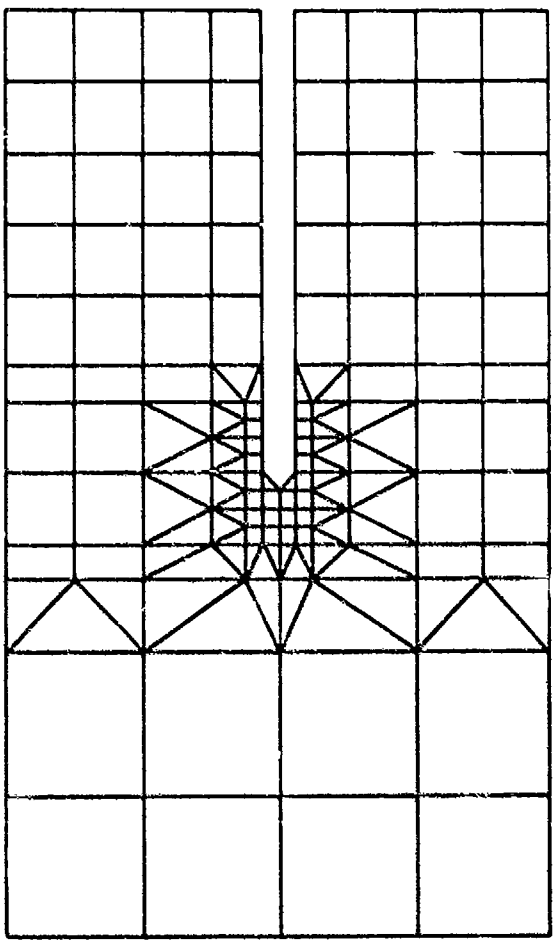

Figure 5. Typical Grid Pattern, a/W = 0.5

mesh be regenerated each time a new crack length was considered. In order to decrease the amount of time spent in regridding the model, a grid generation code obtained from another finite element program (SAAS-Stress Analysis of Axisymmetric Solids)[6] was modified to grid the specimen. The modification and required input into this program is discussed in detail in Appendix C. Briefly, this program interpolates the position of internal nodal points from those specified on the external boundaries. The program then eliminates nodal points as described in Appendix C in order to achieve the desired reduction of the grid pattern. Finally, the element information is obtained by using generated nodal point data.

3.3 Model Geometry

A list of the parameters considered in this investigation is given in Table I. The ratio of crack length to specimen height, a/W, was varied from 0.1 to 0.8. This range was selected to determine the effect that the model boundaries have on the Mode II stress intensity factors for short and long cracks. The dependence of the Mode II stress intensity factor on distance from the load point to crack flank was studied by changing the tang width, H, of the specimen. Three widths were considered; $H = 1.5$ inches, $H = 1.0$ inch, and $H = 0.5$ inch. For $H = 1.5$ inches, the same grid pattern utilized for $H = 1.0$ inch was adopted with the outer boundary elements expanded to give the desired tang width. The grid pattern for $H = 0.5$ inch had to be regenerated. This was easily accomplished by a modification of the griding program which allowed it to accept data for $H = 1.0$ inch, and grid the model

TABLE I

MODEL PARAMETERS USED IN THE INVESTIGATION

H (INCHES)	a/W	W (INCHES)	B (INCHES)
0.5	0.2	3.115	1.00
0.5	0.3	3.115	1.00
0.5	0.5	3.115	1.00
0.5	0.7	3.115	1.00
1.00	0.1	3.115	1.00
1.00	0.2	3.115	1.00
1.00	0.3	3.115	1.00
1.00	0.4	3.115	1.00
1.00	0.5	3.115	1.00
1.00	0.6	3.115	1.00
1.00	0.7	3.115	1.00
1.00	0.8	3.115	1.00
1.50	0.2	3.115	1.00
1.50	0.4	3.115	1.00
1.50	0.5	3.115	1.00
1.50	0.6	3.115	1.00
1.50	0.7	3.115	1.00
1.50	0.8	3.115	1.00

for H = 0.5 inch. The modification restricted the range over which the program will search for nodal points, thus giving the desired tang width.

3.4 Load and Boundary Conditions

The loading conditions used in this investigation consisted of point and uniform loads applied to the specimen as shown in Figures 6a and 6b, respectively. In order to simulate the loading conditions used in the boundary collocation analysis [1], it was necessary to pin the load points in the y-direction as shown in Figure 6a. The left boundary of the model was pinned in the y-direction because it is a line of symmetry. The uniform loading condition, with the nodal points on the upper boundary pinned in the y-direction as shown in Figure 6b, was selected to simulate a fixed grip loading frame. The crack tip was pinned in the z-direction to eliminate any rigid-body movement of the crack flanks in the z-direction.

3.5 Verification of Gridding Program and Numerical Techniques

Verification of the gridding program and numerical techniques for obtaining stress intensity factors was accomplished by generating a representative grid pattern and loading the compact shear specimen as a compact tension specimen. The transformation from compact shear to compact tension specimen was easily made by simply applying the loads at the side and vertical axis of symmetry along a line perpendicular to the crack axis as shown in Figure 7. The Mode I stress intensity factor was then numerically obtained using both the displacement and strain energy release rate techniques and compared to an available closed form

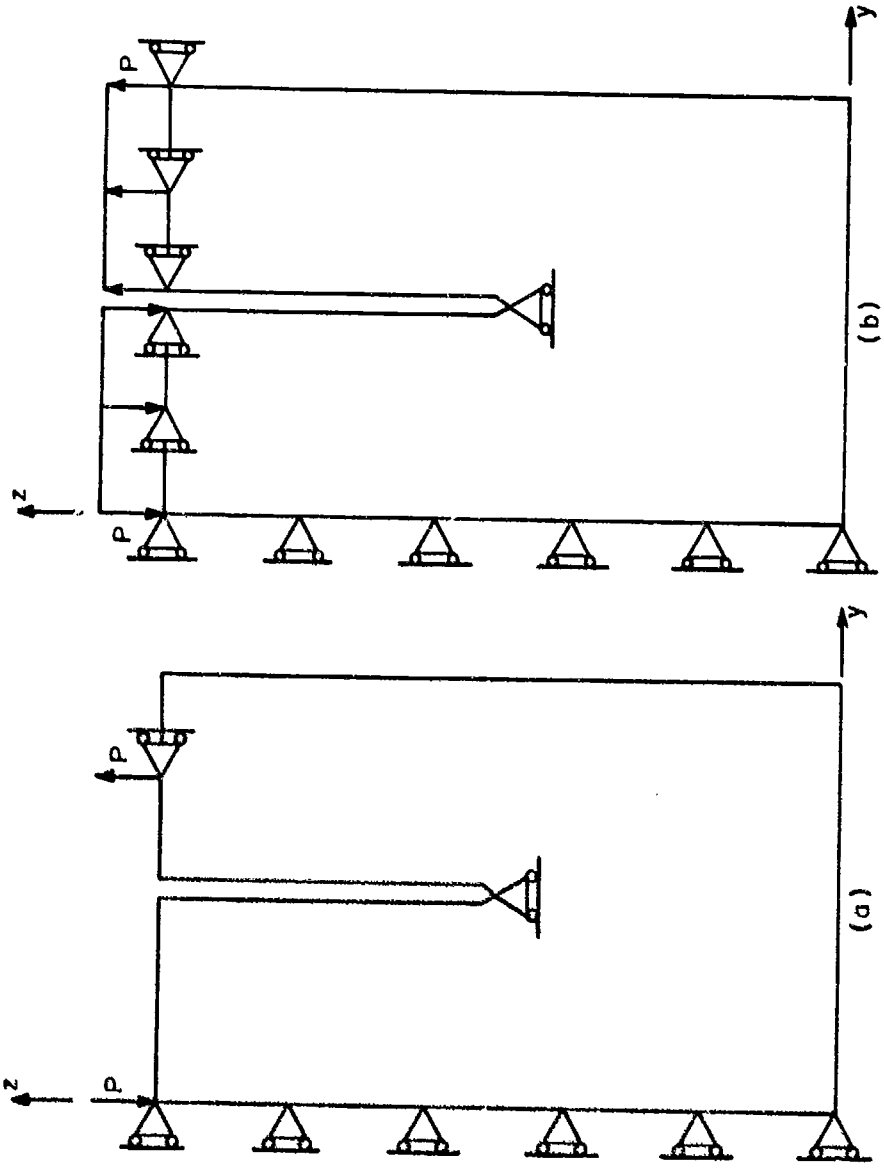

Figure 6. Boundary Conditions for (a) Point Load with Center Point of Tangs Fixed (b) Uniform Load with Upper Tang Boundary Fixed

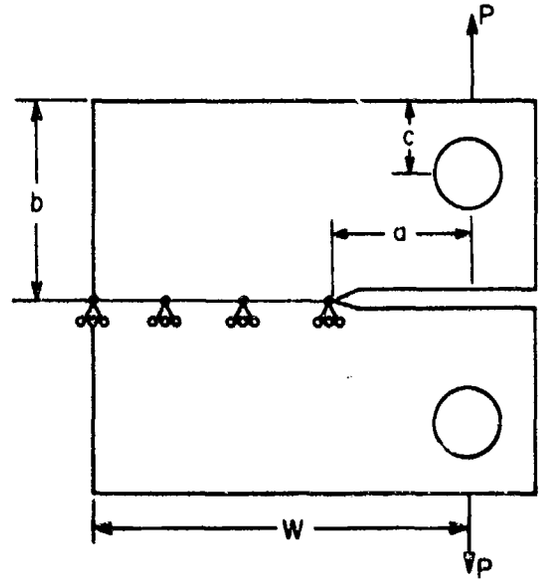

Figure 7. Compact Tension Specimen

solution. A closed form solution for the compact tension specimen, shown in Figure 7, is given by Sih [10] as:

$$k_I = \frac{P(2W + a)}{\sqrt{\pi}\, h(W - a)^{3/2}} \quad F\left(\frac{a}{W}, \frac{b}{W}, \frac{c}{b}\right) \quad . \tag{3.1}$$

where $F\left(\frac{a}{W}, \frac{b}{W}, \frac{c}{b}\right)$ is given for various parameters by Sih [10] and will be used here only for the geometry considered. The boundary conditions necessary for numerical generation of the Mode I stress intensity factor are shown in Figure 7. With these boundary conditions and the model configuration for a compact shear fracture specimen with $a/W = 0.5$ and $H = 1.0$ inch , the physical parameters of Equation (3.1) become

$a = 0.775$ inch

$b = 1.00$ inch

$W = 2.340$ inches

$\frac{c}{b} = 0.3$

$P = 100$ pounds

$h = 1.0$ inch .

A $\frac{c}{b}$ ratio of 0.3 was chosen because this was the closest value listed by Sih which fit the loading conditions applied to the compact tension specimen. It also should be noted that the value of stress intensity factor given by Equation (3.1) is not the same as that determined by the displacement technique. The relation between these two values is given by

$$K_I = \sqrt{\pi}\, k_I \quad , \tag{3.2}$$

where k_I is determined by Equation (3.1) and K_I is determined by the displacement method.

A graph of stress intensity factor versus nondimensionalized distance from the crack tip for the compact tension specimen is given in Figure 8. A least squares fit was performed on the points in the region r/a from 0.1 to 0.2 and K_I, the intercept, was found to be $K_I = 500 \text{ psi}\sqrt{\text{in}}$. The value determined from Equations (3.1) and (3.2) with $F\left(\frac{a}{W}, \frac{b}{W}, \frac{c}{b}\right) = 2.010$ is $K_I = 493 \text{ psi}\sqrt{\text{in}}$. These values are in good agreement with each other and therefore verify the displacement technique and grid generation program.

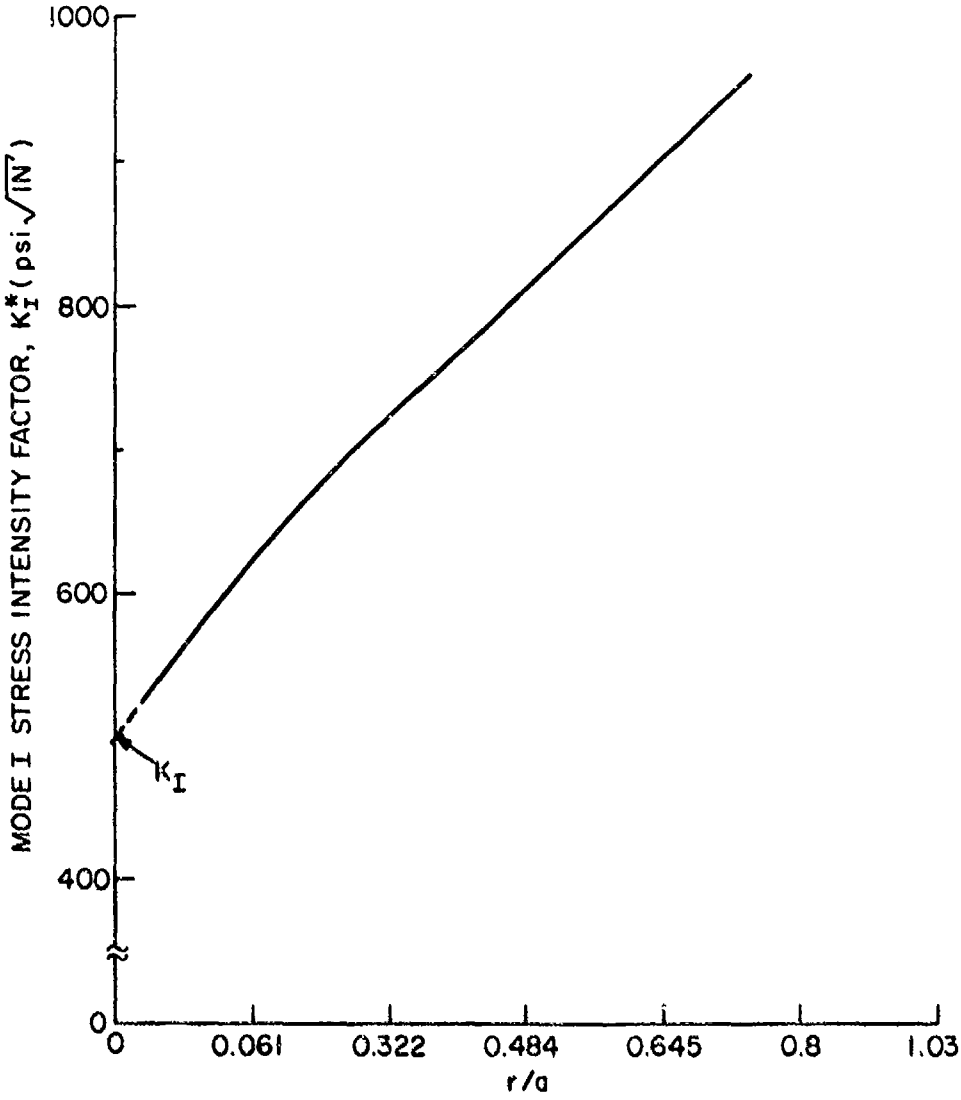

Figure 8. Mode I Stress Intensity Factor Versus r/a for Compact Tension Specimen

CHAPTER IV

ANALYSIS OF RESULTS

4.1 Introduction

Having verified the numerical methods and grid generation program used in this investigation, the behavior of the compact shear fracture specimen as a function of crack length, loading condition and specimen geometry is discussed. Mode II stress intensity factors generated by finite element techniques are compared to those determined by boundary collocation analysis, and to a closed form solution for geometry and loading conditions that closely approximate those of the compact shear fracture specimen. The numerically generated stress distribution on the upper model boundary and vertical axis of symmetry are compared with those assumed by Jones and Chisholm [1] in a boundary collocation study. The initial angle of propagation is also given for selected crack lengths and specimen tang widths.

4.2 Stress Intensity Factors

Numerically generated Mode II stress intensity factors for selected nondimensionalized crack lengths and tang widths are listed in Table II. This data is graphically portrayed in Figure 9 where the Mode II stress intensity factors have been nondimensionalized by dividing K_{II} by the normal stress in the tang, $\sigma = P/BH$, and the square root of crack length, $\sqrt{a}$. The curves shown in Figure 9

TABLE II

NUMERICALLY GENERATED MODE II
STRESS INTENSITY FACTORS

a/W	Mode II Stress Intensity Factors (psi $\sqrt{in.}$)					
	H = 0.5 Inch		H = 1.00 Inch		H = 1.50 Inches	
	Displacement	Energy	Displacement	Energy	Displacement	Energy
0.1	-	-	63.29	58.35	-	-
0.2	148.09	137.30	78.59	69.00	97.21	46.52
0.3	152.49	145.10	92.80	92.50	-	-
0.4	-	-	115.83	107.00	101.69	92.90
0.5	137.68	136.70	122.06	118.00	114.71	107.00
0.6	-	-	145.85	139.00	142.41	129.50
0.7	158.44	166.44	173.09	164.00	169.48	152.40
0.8	-	-	209.27	199.79	-	-

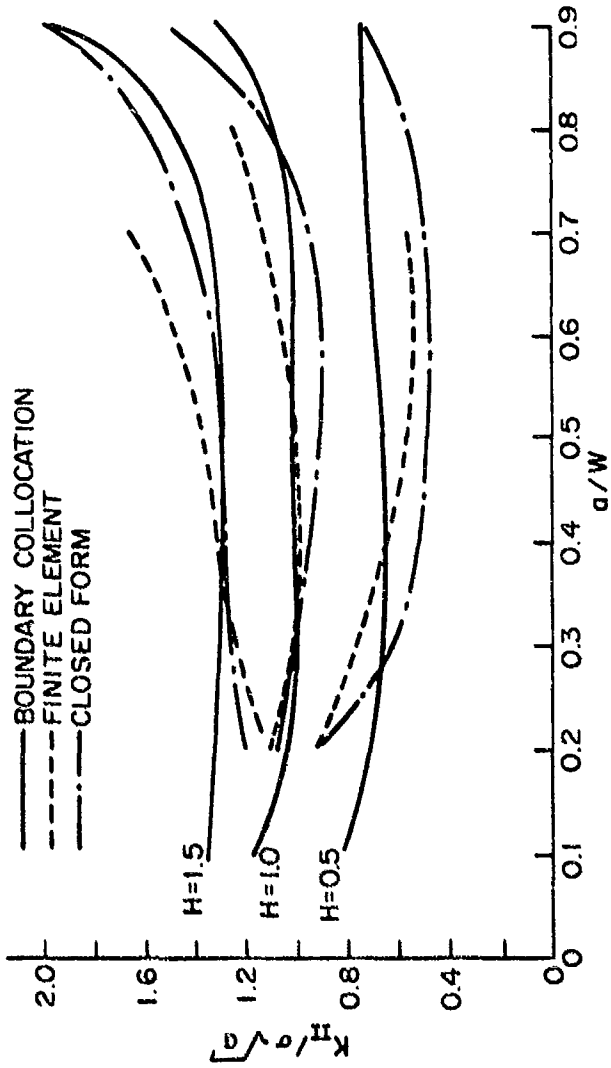

Figure 9. Nondimensionalized Mode II Stress Intensity Factor Versus a/W Ration for Selected Tang Widths H

indicate that the specimen having a tang width $H = 1.0$ inch is the most stable, as evidenced by a relatively constant nondimensionalized Mode II stress intensity factor. The curves for $H = 0.5$ inch and $H = 1.5$ inches exhibit rather wide variations in the nondimensionalized Mode II stress intensity factors with varying crack length. These cases will, therefore be examined in more detail.

Figure 10 shows the variation of the nondimensionalized Mode II stress intensity factor with crack length for a tang width $H = 0.5$ inch. Excellent correlation is shown between results obtained by finite element techniques and those determined from a closed form solution [7]. However, the boundary collocation data does not agree with the numerical and closed form results. The curves for the finite element and closed form solutions show a region of constant nondimensionalized Mode II stress intensity factors from $a/W = 0.4$ to $a/W = 0.7$. For a/W ratios greater than 0.7, the lower specimen boundary influencies the Mode II stress intensity factors. At a/W ratios lower than 0.4, the curves show a load dependence as the load is now being applied close to the crack tip. The boundary collocation curve exhibits constant nondimensionalized Mode II stress intensity factors over the entire range of a/W ratios because of incorrect stress boundary conditions assumed in the boundary collocation analysis. This error in assumed stress boundary conditions will be discussed in detail in a later section.

Figure 11 shows the variation of nondimensionalized Mode II stress intensity factors with crack length for a tang width $H = 1.0$ inch. All curves are in good agreement with each other and have a region of constant nondimensionalized Mode II stress intensity factors

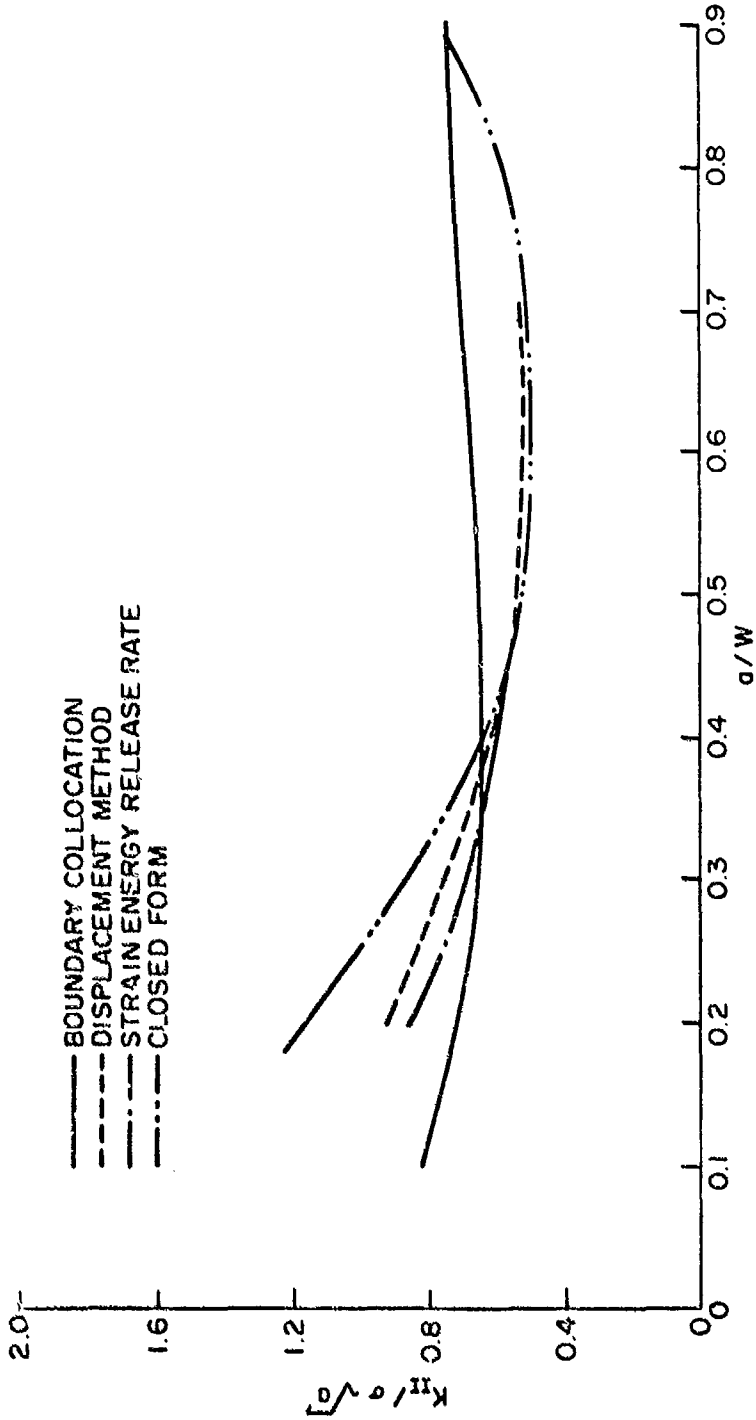

Figure 10. Nondimensionalized Mode II Stress Intensity Factor Versus a/W Ratio for a Tang Width H = 0.5 Inches

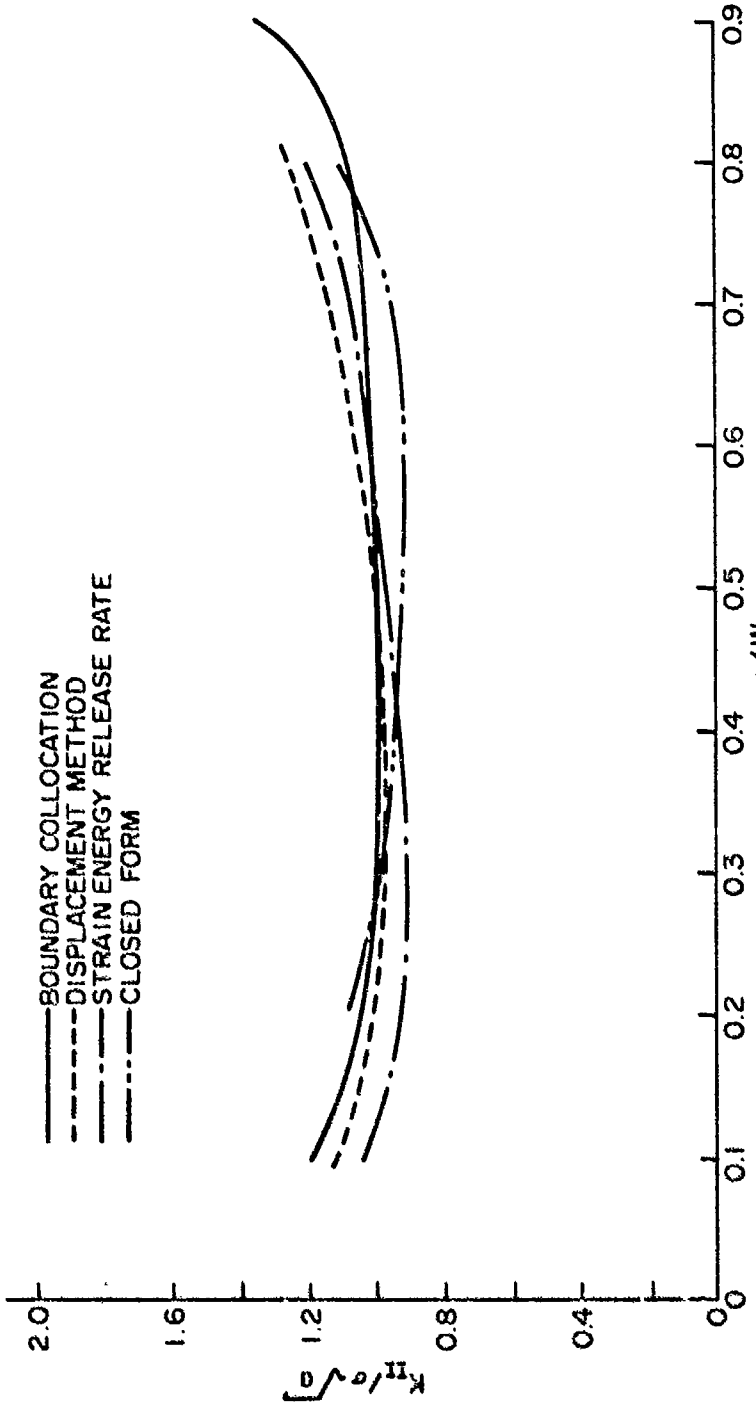

Figure 11. Nondimensionalized Mode II Stress Intensity Factor Versus a/W Ratio for a Tang Width H = 1.0 Inch

from $a/W = 0.2$ to $a/W = 0.6$. At a/W ratios above 0.6 and below 0.2, the specimen boundaries are being sensed by the crack tip, causing the curves to turn upward.

Figure 12 gives the variation of nondimensionalized Mode II stress intensity factors with crack length for a tang width $H = 1.5$ inches. The finite element and closed form results do not exhibit a region over which the nondimensionalized Mode II stress intensity factors are constant because the specimen is now behaving like a beam in three point bending. The influence of bending is evident at all a/W ratios particularly those less than $a/W = 0.3$, for in this region the curves were expected to turn upward as the crack tip sensed the upper boundary of the specimen. The boundary collocation data exhibits a different behavior from that of the finite element and closed form results because of incorrect stress boundary conditions assumed in the boundary collocation study.

4.3 Stress Boundary Conditions

Stress boundary conditions were determined along the upper boundaries of each tang and along the vertical axis of symmetry in order to check those assumed in the boundary collocation analysis and to provide useful data for future investigations utilizing boundary value techniques. Of particular interest in this investigation was the stress distribution along the upper tang boundary and vertical axis of symmetry for application of a point load with the load points fixed in a direction perpendicular to the direction of loading, as shown in Figure 6a. This method of loading was of interest because it simulates that used by

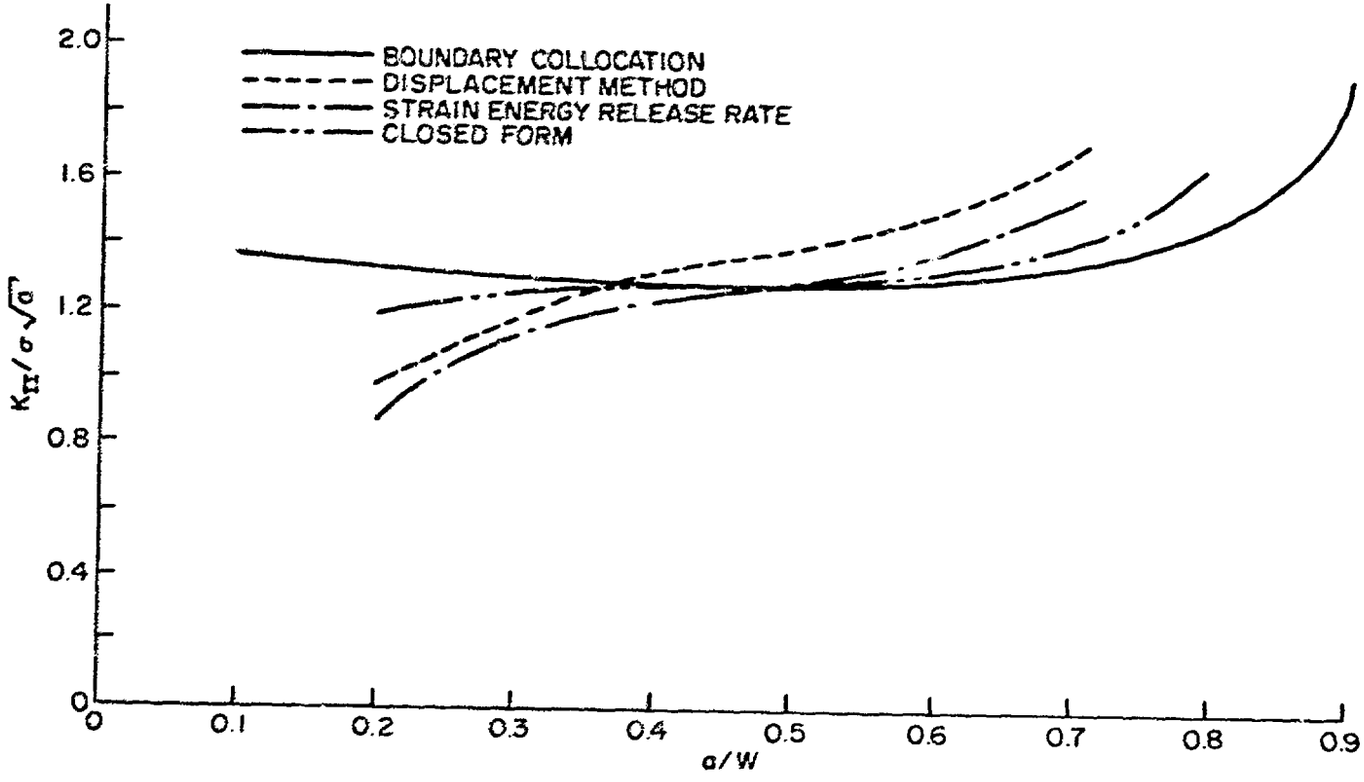

Figure 12. Nondimensionalized Mode II Stress Intensity Factors Versus a/W Ratio for a Tang Width H = 1.5 Inches

Jones and Chisholm so that resultant numerically generated stress distributions could be used to check the stress boundary conditions assumed by Jones and Chisholm. A uniform load with each nodal point on the upper tang boundary fixed in a direction perpendicular to the direction of loading, as shown in Figure 6b, was also applied in order to determine the stress boundary conditions needed in order to perform boundary value analyses for this common type of loading. The two loading conditions just discussed are obtainable through a rigid loading frame. The stress distribution for two other loading conditions are also discussed in this section. These loading conditions are a point load with all nodal points on the upper tang boundary fixed in a direction perpendicular to the direction of loading, and a uniform load with the center point of each tang fixed in a direction perpendicular to the direction of loading. Although these conditions are easily simulated in a numerical study, they are very difficult to obtain experimentally and were considered in this investigation simply to determine the sensitivity of stress intensity factors to changes in boundary conditions.

The stress boundary conditions assumed in the boundary collocation analysis are shown in Figure 13. The stress discribution along the upper tang boundary consists of a uniform tensile stress on the outside tang, a uniform compressive stress along the center tang and a cosine distribution of tangential stress along the top of both tangs. A bilinear bending stress was assumed along the vertical axis of symmetry.

The numerically generated stress distributions along the upper tang boundary and vertical axis of symmetry for $a/W = 0.5$, $H = 1.0$ inch and plane strain conditions are shown in Figures 14 through 19 for

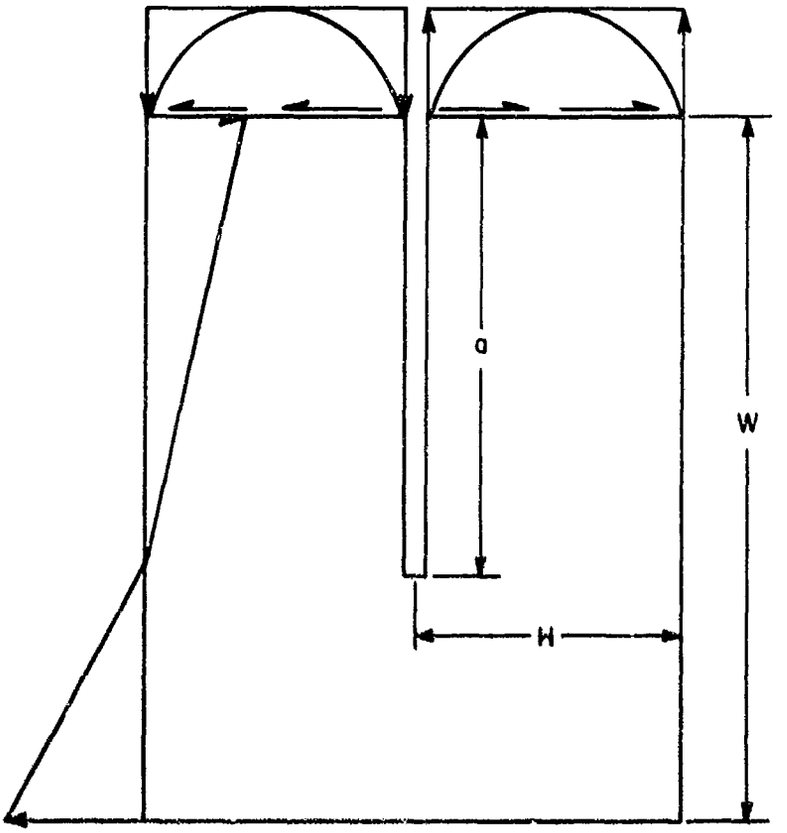

Figure 13. Stress Boundary Conditions Assumed in Boundary Collocation Study

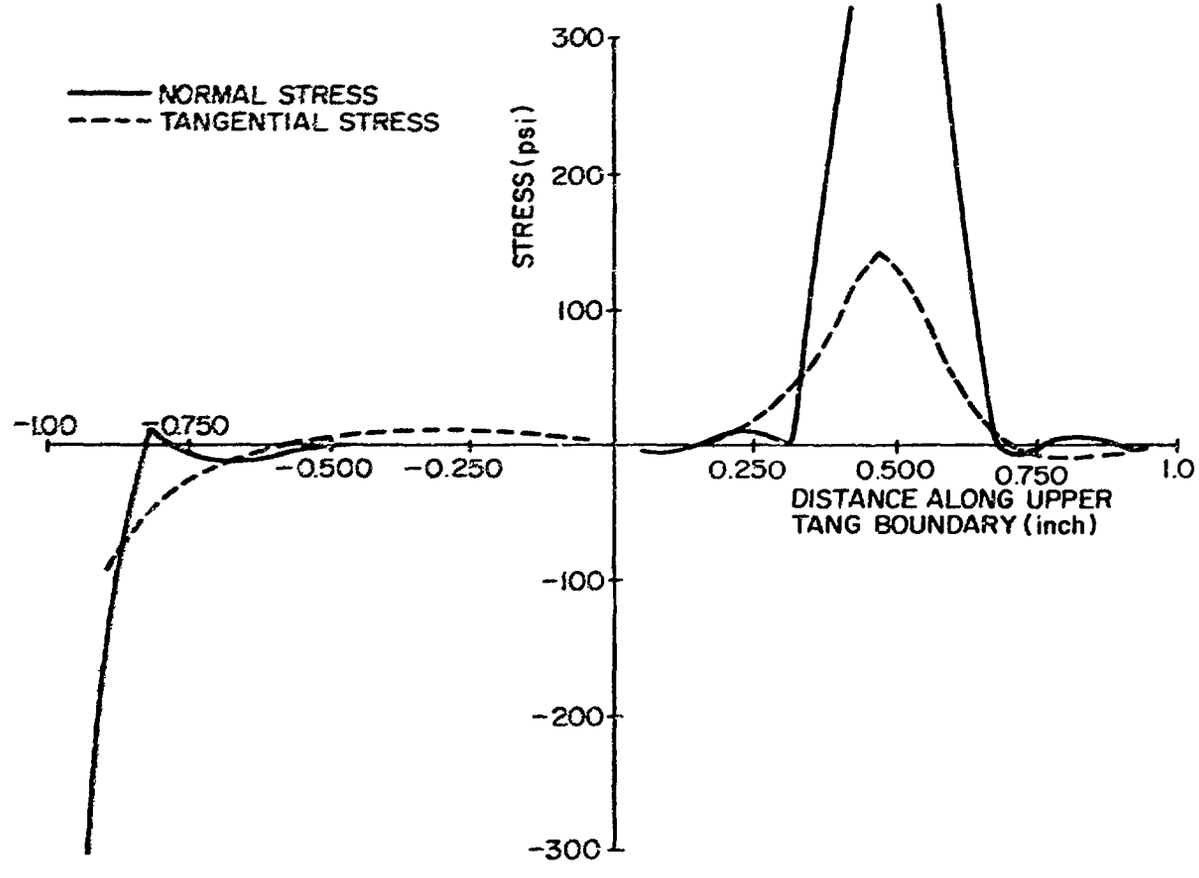

Figure 14. Numerically Generated Stress Distribution Along Upper Tang Boundary for a/W = 0.5, H = 1.0 Inch, Point Load, Center Point of Tangs Fixed, and Plane Strain Conditions

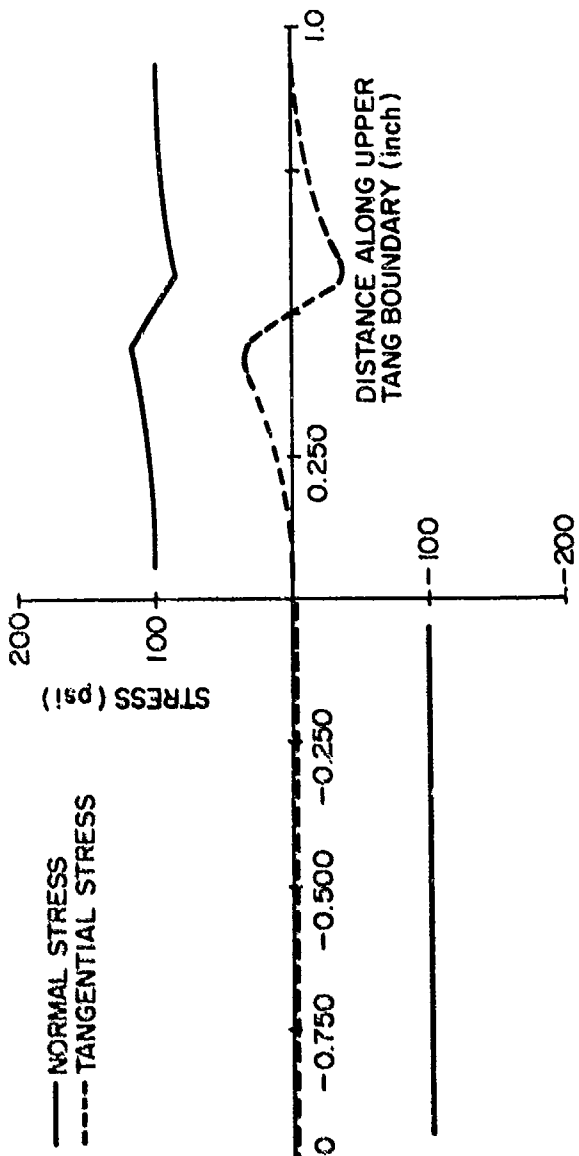

Figure 15. Numerically Generated Stress Distribution Along Upper Tang Boundary for a/W = 0.5, H = 1.0 Inch, Uniform Loading, Center Point of Tangs Fixed, and Plane Strain Conditions

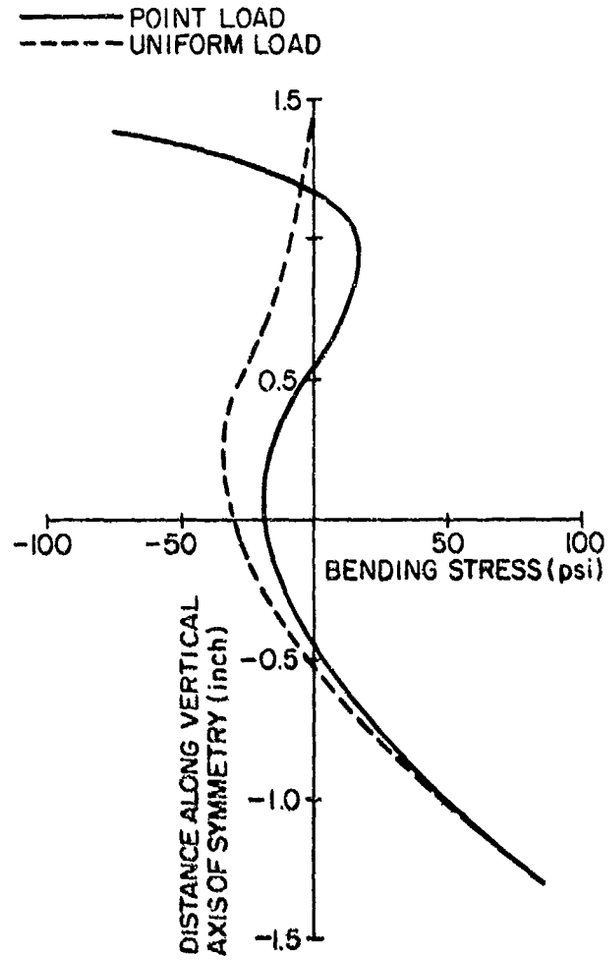

Figure 16. Numerically Generated Stress Distribution Along Vertical Axis of Symmetry for a/W = 0.5, Center Point of Tangs Fixed, and Plane Strain Conditions

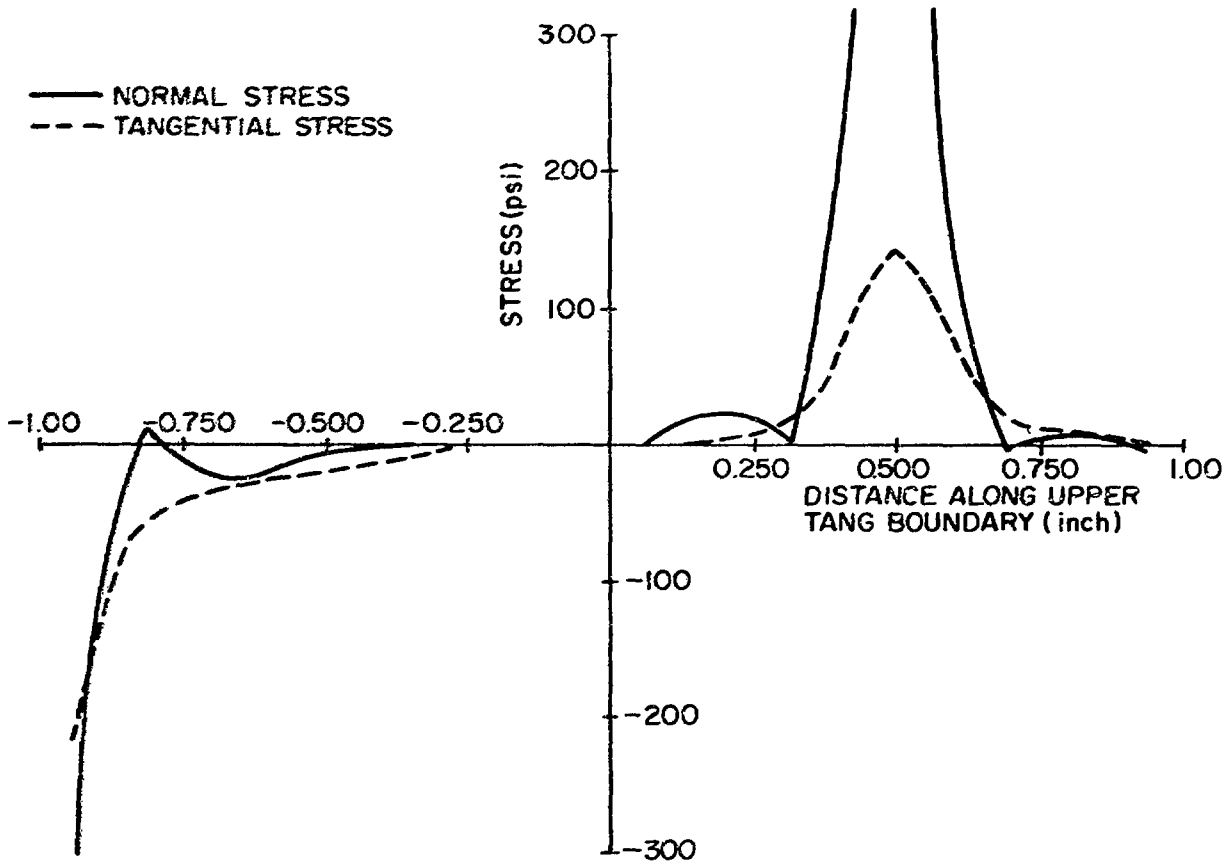

Figure 17. Numerically Generated Stress Distribution Along Upper Tang Boundary for a/W = 0.5, H = 1.0 Inch, Point Load, Upper Tang Boundary Fixed, and Plane Strain Conditions

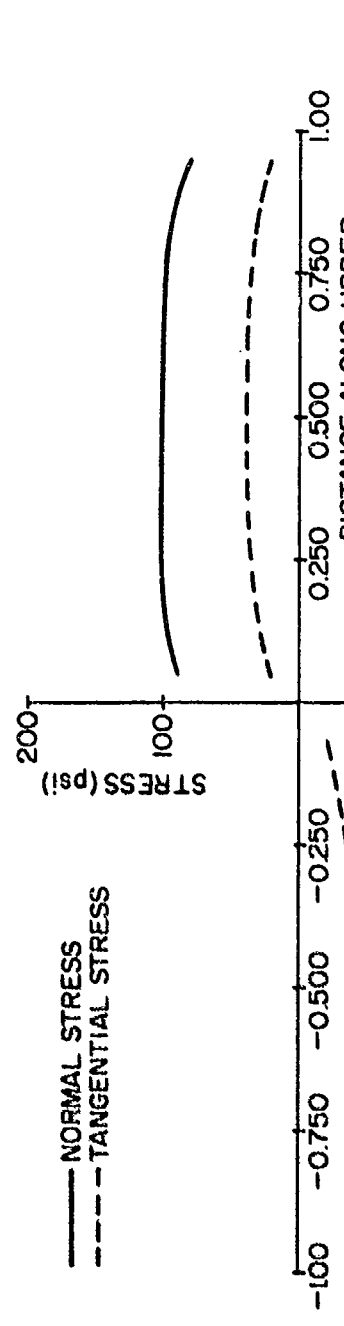

Figure 18. Numerically Generated Stress Distribution Along Upper Tang Boundary for a/W = 0.5, H = 1.0 Inch, Uniform Loading, Upper Tang Boundary Fixed, and Plane Strain Conditions

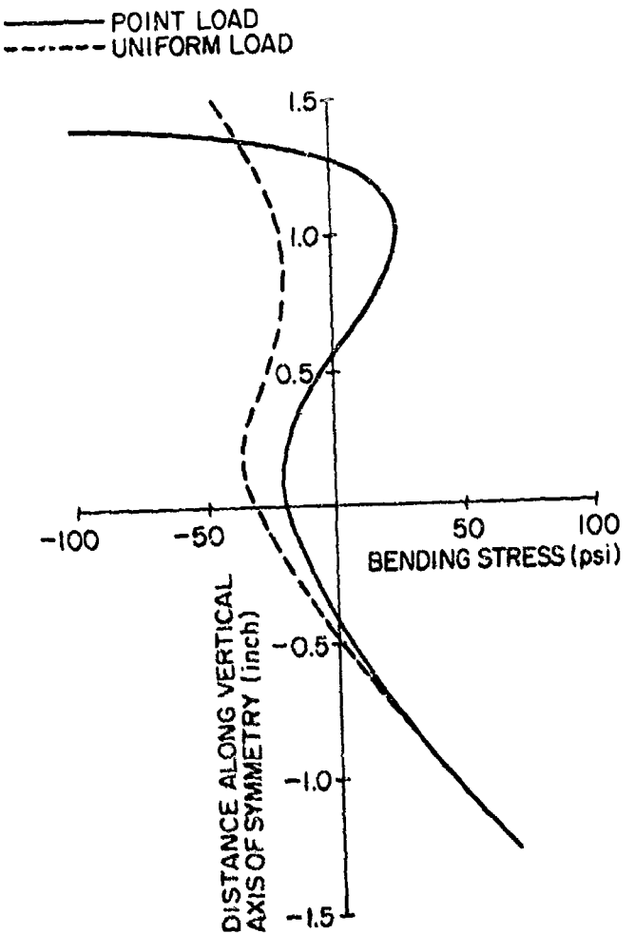

Figure 19. Numerically Generated Stress Distribution Along Vertical Axis of Symmetry for a/W = 0.5, H = 1.0 Inch, Point and Uniform Loading, Upper Tang Boundary Fixed, and Plane Strain Conditions

selected load and displacement boundary conditions. Figures 14 through 16 show the stress distributions for a point and uniform load with the center point of each tang fixed in a direction perpendicular to the direction of loading. Figures 17 through 19 show the stress distributions for a point and uniform load with each nodal point along the upper tang boundary fixed in a direction perpendicular to the direction of applied load.

As can be seen by referring to Figures 14 and 17, the normal and tangential stress distribution along the upper tang boundaries caused by the application of a point load does not change as the displacement boundary conditions are varied. Figures 15 and 18 show that the tangential stress distribution along the upper tang boundaries caused by the application of a uniform load is in fact the only distribution affected by variation in displacement boundary conditions. Figures 16 and 19 show practically no change in the normal stress distribution along the vertical axis of symmetry for variation in displacement boundary conditions.

Comparison of Figures 13, 14 and 17 indicates that the numerically generated stress distributions for point loading are not in good agreement with those assumed in the boundary collocation analysis. The major differences occur in the normal stress distribution along the upper tang boundary. This difference in stress distribution is responsible for the discrepancies observed in the nondimensionalized Mode II stress intensity factors determined by numerical techniques and boundary collocation analysis.

The stress distributions caused by the application of a uniform load with all the nodal points along the upper tang boundary fixed, as shown in Figure 18, were somewhat similar to those assumed in the boundary collocation analysis, shown in Figure 13. The major difference in the two distributions is that the numerically generated tangential stress distribution on the center tang is not a cosine distribution as assumed in the boundary collocation analysis. Figures 16 and 19 show that the bending stress along the vertical axis of symmetry for both point and uniform loading is not a simple bilinear distribution as shown in Figure 13.

Numerically generated stress distributions were also obtained for other a/W ratios and tang widths resulting in distributions having the same form but different magnitudes then those shown in this section. Plane stress conditions were also tried for selected load conditions and model geometries resulting in no difference in stress distributions when compared to those determined using plane strain conditions. The Mode II stress intensity factors were unaffected by changes in loading and displacement boundary conditions discussed in this section.

4.4 Initial Angle of Crack Propagation

The angle of propagation θ is defined in Figure 3. By use of the strain energy density technique proposed by Sih [5] and discussed in Chapter II, the angle of propagation was determined for $a/W = 0.5$ through 0.8 with $H = 1.0$ inch . These values are listed in Table III. These particular values of crack length and specimen tang width were chosen because the experimental work performed by Jones considered an

TABLE III

NUMERICALLY PREDICTED INITIAL ANGLE OF PROPAGATION FOR SELECTED a/W RATIOS WITH A TANG WIDTH H = 1.00 INCH

a/W	THETA θ
0.5	77°
0.6	77°
0.7	77°
0.8	75°

a/W .ratio of 0.8 with specimen tang width, H = 1.0 inch . With these parameters, and notching the model along the plane of the crack, Jones and Chisholm were able to obtain a straight fracture of the specimen, $\theta = 0°$. As can be seen from Table III, the strain energy density technique predicts that the initial angle of propagation is 75° for $a/W = 0.8$ and 77° for $a/W = 0.5$ to 0.7 . The path of the crack was not investigated after the initial angle of propagation because of the amount of computer time necessary to accomplish this.

CHAPTER V

CONCLUSIONS AND RECOMMENDATIONS

5.1 Conclusions

The effect of crack length and specimen geometry on the Mode II stress intensity factors for the compact shear fracture specimen shown in Figure 2 was investigated. Stress intensity factors were generated by the displacement and strain energy release rate methods and compared to those determined by boundary collocation. Both numerical and boundary collocation results obtained for a tang width $H = 1.0$ inch show that nondimensionalized Mode II stress intensity factors are constant for this specimen over a wide range of crack lengths. This configuration of the compact shear fracture specimen will therefore be most suitable for determining critical Mode II stress intensity factors, K_{IIc}.

Numerical results for $H = 0.5$ inch and $H = 1.5$ inches show that nondimensionalized Mode II stress intensity factors are not as stable with increasing crack length as the boundary collocation results suggest. The stress intensity factors obtained for a tang width $H = 1.5$ inches are affected by bending of the specimen, a fact that was not brought out by the boundary collocation results. Results for tang width $H = 0.5$ inch indicated that the nondimensionalized Mode II stress intensity factors were influenced by applied load for a/W ratios less than 0.4 . Because of these nonlinearities, the configuration

having tang width H = 0.5 inch and H = 1.5 inches are not suitable for determining the critical Mode II stress intensity factor, K_{IIc}. For the crack lengths and specimen geometries investigated, the non-dimensionalized Mode II stres intensity factors were found to be independent of the applied load, and uninfluenced by the lower free boundary through the intermediate ranges of crack lengths.

Numerical results indicated that the tangential stress along the upper boundary of the center tang did not follow a cosine distribution as assumed in the boundary collocation analysis. In addition the numerically determined bending stress distribution along the vertical axis of symmetry was not found to be the simple bilinear distribution which was used in the boundary collocation investigation. Therefore, incorrect stress boundary conditions assumed in the boundary collocation analysis were responsible for differences observed in the behavior of the nondimensionalized Mode II stress intensity factors when numerical and collocation results are compared.

The initial angle of propagation was found numerically to be 77° for the geometry and crack lengths considered. This differs from the experimental work performed by Jones and Chisholm [1], which showed an angle of 0° of crack propagation. The angle of 0° might have been the result of notching the fracture specimen along the plane of the crack. The difference between the numerically predicted angle of propagation and experimental results might not have been so great if it were possible to numerically determine the complete trajectory of the crack. This was not done because of the amount of computer time involved.

This study also showed the usefullness of the finite element method in determining Mode II stress intensity factors, for different loading conditions and specimen parameters. The accuracy of the finite element techniques discussed in this investigation was brought out by the good agreement with a closed form solution.

5.2 Recommendations

It is recommended that:

1) An experimental verification of the stress boundary conditions and Mode II stress intensity factors predicted by the finite element techniques used in this investigation be performed.

2) A verification of the crack trajectory by experimental or numerical techniques, with a notch introduced into the model for comparison with the experimental work performed by Jones and Chisholm be undertaken.

BIBLIOGRAPHY

1. Jones, D. L. and Chisholm, D. B., "An Investigation of the Edge-Sliding Mode in Fracture Mechanics," School of Engineering and Applied Science, George Washington University, Technical Report, No. 18 (1974).

2. Chan, S. K., Tuba, I. S. and Wilson, W. K., "On the Finite Element Method in Linear Fracture Mechanics," Engineering Fracture Mechanics, Pergamon Press (1970), pp. 1-17.

3. Paris, P. C. and Sih, G. C., "Stress Analysis of Cracks," Fracture Toughness Testing and Its Applications, ASTM STP 381 (1965), pp. 39-76.

4. Experimental Techniques in Fracture Mechanics, Society for Experimental Stress Analysis Monograph, No. 1 (1973), pp. 7-14.

5. Sih, G. C., "Some Basic Problems in Fracture Mechanics and New Concepts," Engineering Fracture Mechanics, Pergamon Press (1973), pp. 365-377.

6. Haney, J. E. and Bannister, K. A., "NWL-SAAS III User's Guide," Naval Weapons Laboratory Technical Note TN-K-61173 (1973).

7. Tada, H., Paris, P. C. and Irwin, G. R., The Stress Analysis of Cracks Handbook, Del Research Corporation (1973).

8. Wilson, E. L., Solid SAP, University of California, Berkley (1972).

9. Desi, C. S. and Abel, J. E., Introduction to the Finite Element Method, Van Nostrand Reinhold (1972).

10. Sih, G. C., Handbook of Stress Intensity Factors for Researchers and Engineers, Lehigh University (1973).

APPENDIX A

FINITE ELEMENT PROGRAM USED IN THE INVESTIGATION

A.1 Finite Element Program

The finite element program utilized in this investigation was SSAP-2 (Static Analysis Program For Solid Structures). A complete listing of the program as well as a description of the elements and input to the program is given in the program manual [8]. A brief description of the plate element used in the study will be given here.

A.2 Isoparametric Elements

A isoparametric element [9] is defined as one where both the displacement and geometry of the element are described by the same parameter. This means that the relation between the local and global coordinate systems as well as the displacement approximation for the element are given in terms of the same interpolation function. An interpolation function is one that has a unit value at one nodal point and is zero at all others in the element. Two advantages of using interpolation functions are:

1) If continuity of geometry and displacement both within and between adjacent elements are satisfied, compatibility is satisfied in global coordinates.

2) If the interpolation function is able to give rigid body displacements in the local coordinate system, rigid body displacement

and constant strain are satisfied in the global system. This is necessary for convergence of the method.

The interpolation functions used in SSAP will now be discussed. For the quadrilateral element shown in Figures 20 and 21 the local and global coordinates are related by

$$x = \sum_{i=1}^{4} h_i x_i$$

and (A.1)

$$y = \sum_{i=1}^{4} h_i y_i \quad ,$$

where the interpolation functions, h_i , are given as:

$$h_1 = \frac{1}{4}(1 - s)(1 - t) \quad ,$$

$$h_2 = \frac{1}{4}(1 + s)(1 - t) \quad ,$$

$$h_3 = \frac{1}{4}(1 + s)(1 + t) \qquad (A.2)$$

and

$$h_4 = \frac{1}{4}(1 - s)(1 + t) \quad ,$$

where s and t are defined in Figure 21.

The displacements of the element are written in terms of the same interpolation functions as follows:

$$u_x(s,t) = \sum_{i=1}^{4} h_i u_{xi}$$

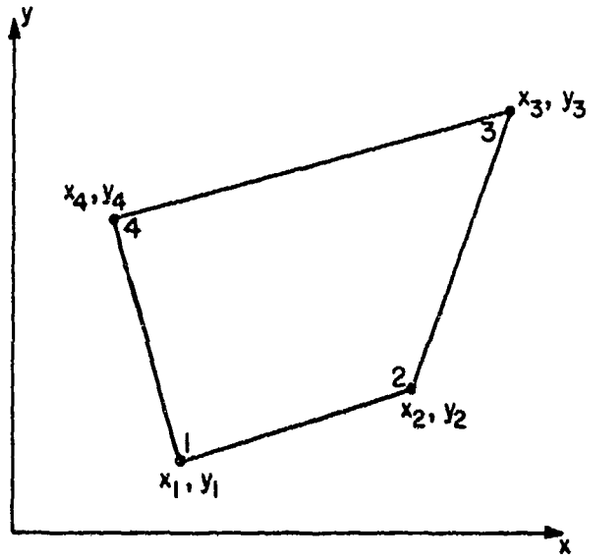

Figure 20. Global Coordinate System Used in SSAP

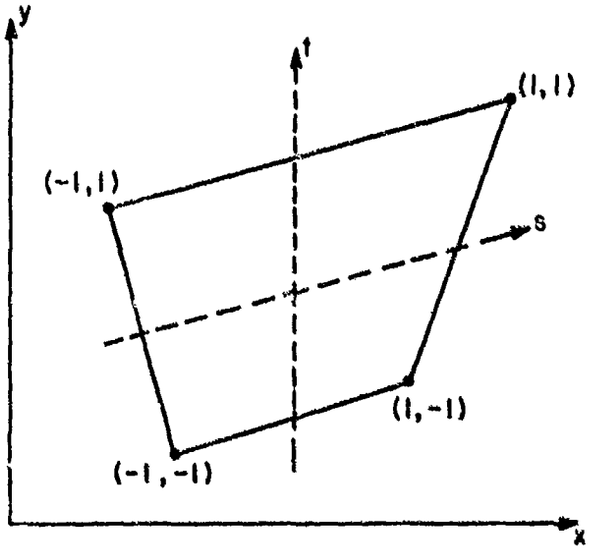

Figure 21. Local Coordinate System Used in SSAP

and

$$u_y(s,t) = \sum_{i=1}^{4} h_i u_{yi} \quad . \tag{A.3}$$

The element strains can now be written as

$$\varepsilon_{xx} = \frac{\partial u_x}{\partial x} = \sum_{i=1}^{4} h_{i,x} u_{xi} \quad ,$$

$$\varepsilon_{yy} = \frac{\partial u_y}{\partial y} = \sum_{i=1}^{4} h_{i,y} u_{yi} \tag{A.4}$$

and

$$\varepsilon_{xy} = \frac{\partial u_y}{\partial y} + \frac{\partial u_y}{\partial x} = \sum_{i=1}^{4} h_{i,y} u_{xi} + \sum_{i=1}^{4} h_{i,x} u_{yi} \quad .$$

These equations can be written in matrix form as:

$$\underline{\varepsilon} = \underline{a}(s,t)\underline{u} = \begin{bmatrix} H_{,x} & 0 \\ 0 & H_{,y} \\ H_{,y} & H_{,x} \end{bmatrix} \begin{bmatrix} \underline{u_x} \\ \\ \underline{u_y} \end{bmatrix} \quad , \tag{A.5}$$

where $\underline{u_x}$ and $\underline{u_y}$ are the displacements in the x and y directions, respectively and

$$H_{,x} = [h_{1,x} \; h_{2,x} \; h_{3,x} \; h_{4,x}]$$

and

$$H_{,y} = [h_{1,y} \; h_{2,y} \; h_{3,y} \; h_{4,y}] \quad , \tag{A.6}$$

where

$$h_{i,x} = h_{i,s} \, s_{,x} + t_{i,t} \, t_{,x}$$

and

$$h_{i,y} = h_{i,s} \, s_{,y} + h_{i,t} \, t_{,y} \quad .$$

Since the h_i are given in terms of the natural coordinates, s and t, the chain rule must be applied in order to compute the derivatives in terms of the x and y coordinate system. The result of the application of the chain rule is shown in matrix form below as:

$$\begin{bmatrix} s_{,x} & t_{,x} \\ s_{,y} & t_{,y} \end{bmatrix} = \frac{1}{J} \begin{bmatrix} y_{,t} & -y_{,s} \\ -x_{,t} & x_{,s} \end{bmatrix} , \tag{A.7}$$

where J is the Jacobian which is defined by

$$J = x_{,s}\, y_{,t} - x_{,t}\, y_{,s} ,$$

$$x_{,s} = \sum_{i=1}^{4} h_{i,s}\, x_i ,$$

$$x_{,t} = \sum_{i=1}^{4} h_{i,t}\, x_i , \tag{A.8}$$

$$y_{,s} = \sum_{i=1}^{4} h_{i,s}\, y_i$$

and

$$y_{,t} = \sum_{i=1}^{4} h_{i,t}\, y_i .$$

Now Equations (A.7) and (A.8) can be used with Equations (A.6) to determine the strain-displacement matrix of Equation (A.5).

A.3 Element Stiffness

The element stiffness for unit thickness is given as

$$\underline{K} = \int \underline{a}^T \underline{c}\, \underline{a}\, dA . \tag{A.9}$$

$\underline{c}$ is the stress-strain matrix and the integration is performed over the area of the element. This equation can be written in terms of the natural coordinate system as

$$\underline{K} = \int_{-1}^{1}\int_{-1}^{1} \underline{a}^T \underline{c}\, \underline{a}\, J \, ds \, dt \quad . \tag{A.10}$$

Standard numerical integration is used to determine $\underline{K}$ for a given element.

A.4 Total Stiffness Matrix

Once the element stiffnesses have been determined, the total stiffness matrix is obtained by summing element stiffnesses in the conventional manner,

$$\underline{K}_{TOTAL} = \Sigma \underline{K}_{ELEMENT} \quad . \tag{A.11}$$

A complete description of the finite element method is given by Desi [9].

APPENDIX B

CLOSED FORM SOLUTION

B.1 Geometry and Equations

The verification of the finite element results was accomplished by comparison with a closed form solution for a model with geometry and loading conditions similar to those of the compact shear fracture specimen being studied. Since a geometry and loading condition that exactly matched this model was not available, a configuration was considered that would give a lower bound to the finite element results. The loading, geometry and closed form solution were chosen from a handbook by Tada [7] and the model is shown in Figure 22. This configuration was chosen because the loading applied is similar to the loading on the compact shear fracture specimen. The configuration will give a lower bound to the problem because it is an infinite strip and therefore stiffer than the actual plate. The equations for the Mode II stress intensity factor, K_{II} , are given below:

$$K_{II} = \frac{Q}{\sqrt{2b}} \{F_{II}(\frac{a}{b}, \frac{s}{b})\} \quad , \tag{B.1}$$

where

$$F_{II}(\frac{a}{b}, \frac{s}{b}) = f(\frac{a}{b}, \frac{s}{b}) \left[1 - \frac{\alpha \frac{\pi s}{2b} \tanh \frac{\pi s}{2b}}{\left[\frac{\cosh \frac{\pi s}{2b}}{\cos \frac{\pi a}{2b}} \right]^2 - 1} \right] F_{III}(\frac{a}{b}, \frac{s}{b}) \quad , \tag{B.2}$$

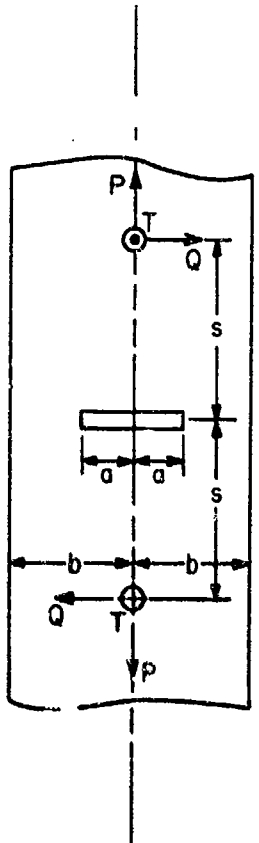

Figure 22. Center Cracked Infinite Strip Used in Closed Form Solution

$$F_{III}\left(\frac{a}{b}, \frac{s}{b}\right) = \left\{ \sqrt{\tan \frac{\pi a}{2b}} \right\} \frac{1}{\sqrt{1 - \left[\frac{\cos \frac{\pi a}{2b}}{\cosh \frac{\pi s}{2b}} \right]^2}} , \qquad (B.3)$$

$$f\left(\frac{a}{b}, \frac{s}{b}\right) = 1 + \{0.297 + 0.115(1 - \operatorname{sech} \frac{\pi s}{2b}) \sin \frac{\pi a}{b}\} (1 - \cos \frac{\pi a}{2b}) \qquad (B.4)$$

and

$$\alpha = \begin{cases} \frac{1 + \nu}{2} & \text{plane stress} \\ \\ \frac{1}{2(1 - \nu)} & \text{plane strain} \end{cases} . \qquad (B.5)$$

APPENDIX C

GRID GENERATION

C.1 Introduction

The mesh generation program utilized in this investigation is a modified version of one used in SAAS [6]. The modification is in the element generation subroutine and nodal point interpolation. Element generation was changed in order to generate triangular elements in regions of transition from course to fine gridding and nodal point interpolation was modified to make grid reduction possible.

C.2 Input Required

Input into the gridding program will be described by considering the gridding of a plate with a notch as shown in Figure 23. The requirements for gridding a crack problem, without the use of special crack tip elements, are that a fine grid be placed in the crack tip region to accommodate the high stress gradient there. Also, in order to save computer time and storage, a relatively course grid should be applied at the boundaries. These two requirements can be accomplished by a transition region of triangular elements. The procedure for obtaining input data for this program is as follows. Determine what type of grid pattern is needed at the crack tip, using only quadralateral elements. This will give a very fine element distribution as shown in Figure 24. Each horizontal line with the same z-coordinate is

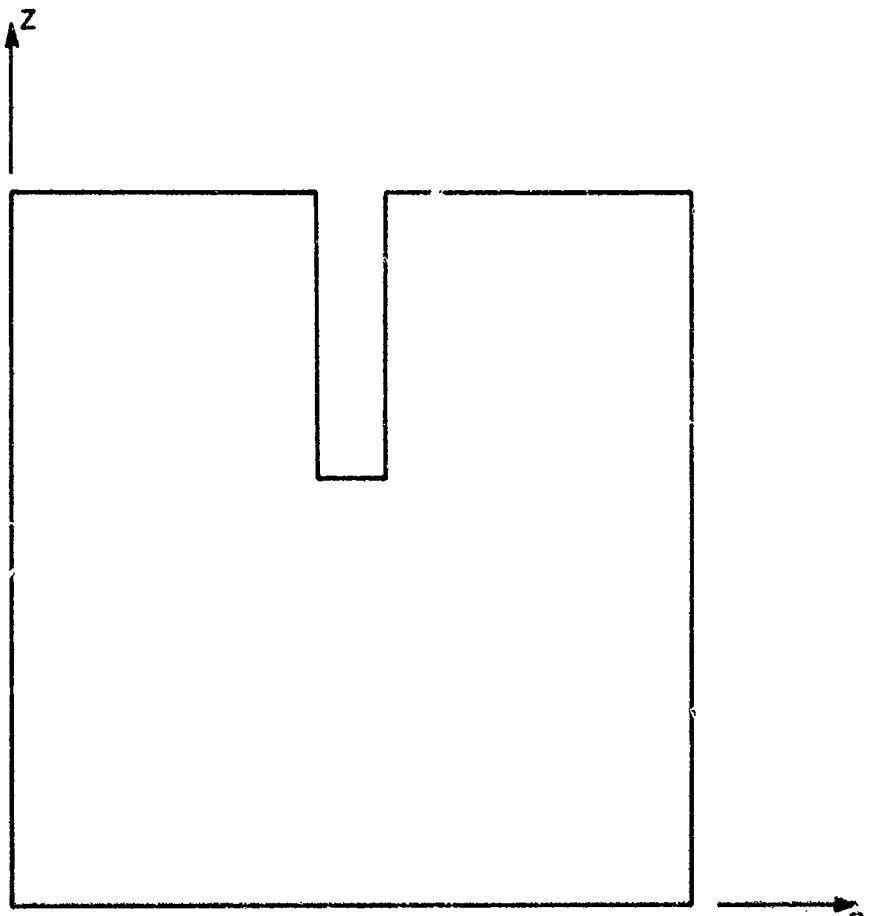

Figure 23. Notched Plate Used in Sample Problem

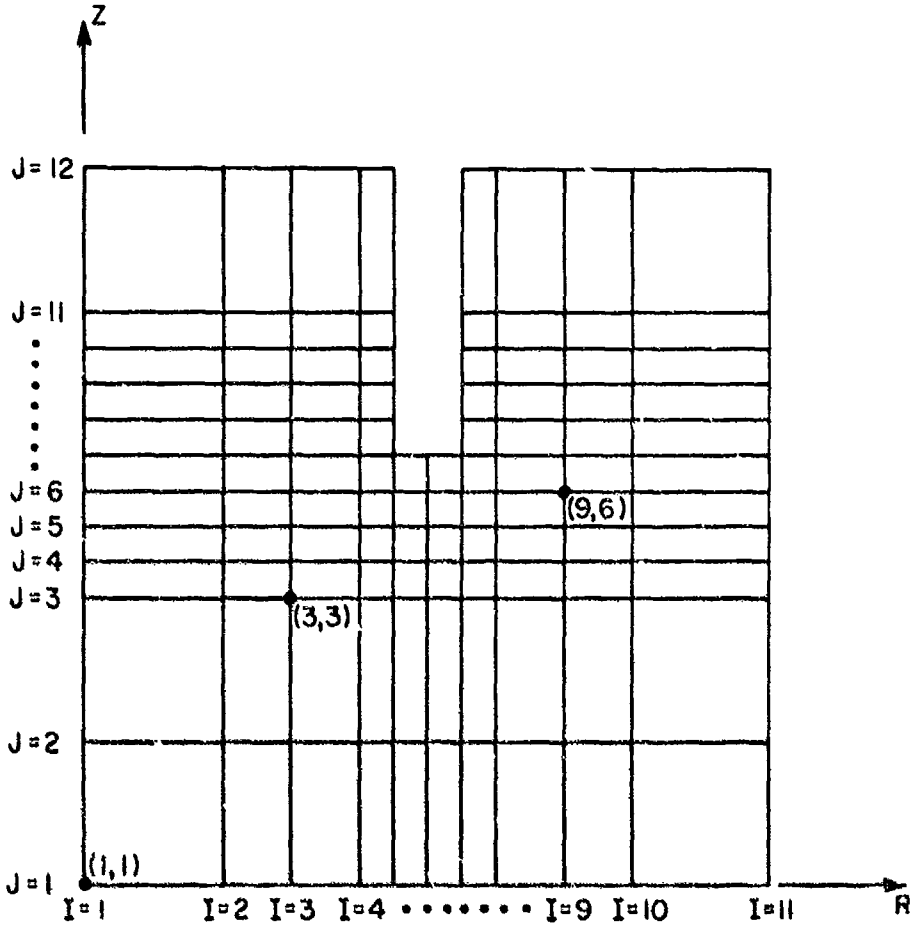

Figure 24. Grid Pattern for Notched Plate Without Triangular Transition Elements

assigned a J index to identify it, starting with the $z = 0$ line. The same is done with every vertical line with the same R coordinate, except these are assigned I indices; therefore, every intersection, nodal point, has an I,J index to identify it. The transition can now be accomplished by eliminating sections of J rows and I columns in order to achieve the desired grid pattern. The only restriction is that a section of eliminated J row cannot intersect a portion of I column that will be eliminated because the program will not be able to generate a valid element. Figure 25 shows a completed grid pattern.

The sequencing of the input data will now be described. A listing of input data for this problem is given in Figure 26. The first three cards are control cards and are described in the manual for SAAS and the control data for the finite element program has been eliminated. The cards and formating are described below.

Title Card

Describe grid pattern

Format (8A10)

Columns 1-60 Title

Job Control Card

Format (I2, I3, I5, I2, I3, 5I5, I3, I2, 2I5, I5.0, 3I5)

Columns 3-5 Start parameter

= 1 Fresh set of data

Columns 6-10 Stop parameter

= 1 Stop after mesh generation

= 33 Punch mesh data on cards

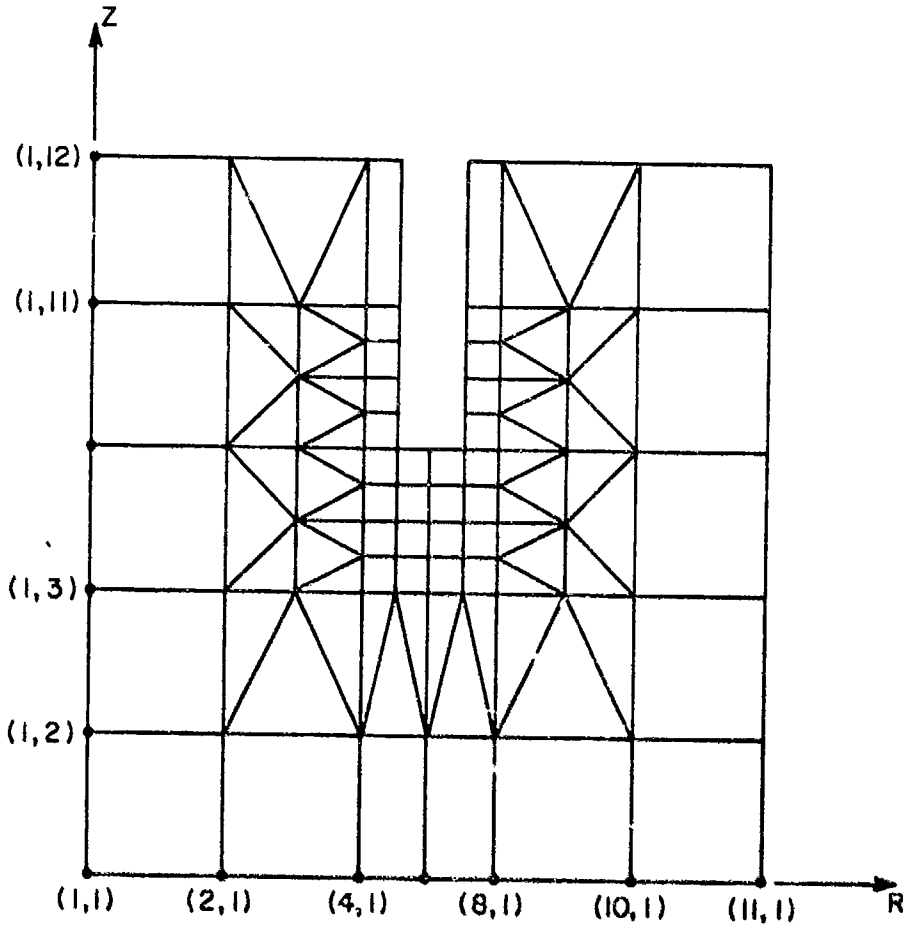

Figure 25. Completed Grid Pattern for Notched Plate

```
SAMPLE PROBLEM: NOTCHED PLATE
1  1     1                    1           1
 400           1
 1   1 0.0     0.0                                    1
 2   1 1.000    0.0                                   1
 4   1 2.000    0.0                                   1
 8   1 3.000    0.0                                   1
10   1 4.000    0.0                                   1
11   1 5.000    0.0                                   1
 1   1 0.0      0.0                                  -1
 1   3 0.0      2.000                                 1
 1  11 0.0      4.000                                 1
 1  12 0.0      5.000                                 1
-2
  11    12     5     6     6     7
   1     3     7    11    12

 2.5000    3.000
   6
   4     4     8
   5     3     9
   6     4     8
   8     4     8
   9     3     9
  10     4     8
   4
   3     3    11
   5     3    12
   7     3    12
   9     3    11
  11     5     3
   1     1    11     1    12
```

Figure 26. Listing of Input to Grid Generation Program for Notched Plate

Columns 21-25 Finite element mesh generation parameter

≠ 0 Generate mesh using line segment data

= 0 Mesh data read from cards

Columns 26-30 Temperature field

= 0 Must be set equal to zero

Columns 31-34 Number of materials (6 maximum)

These are the only parameters needed to generate a mesh, the rest can be set equal to zero.

Mesh Generation Card

Format (4I5, 2F10.0, 2I5)

Columns 1-5 Number of line segment cards. The actual number of cards may be less than this, as long as a line segment terminator card follows them.

Columns 11-15 Number of material assignment cards

Line Segment Cards

They describe the boundary of the model.

Format (2I3, 2F8.3, I5)

Columns 1-3 I2 (or I1 if this is the first card)

I - index of point

Columns 4-6 J2 (or J1 if first card)

J - index of point

Columns 7-14 R2 R coordinate of point

Columns 15-22 Z2 Z coordinate of point

Columns 45-49 IPTION Integer value that determines type of line segment

IPTION	Description of Line Segment
-1	Jump to this point from last, no mesh data will be generated and no line will connect the points.
0	Same as -1 except a line will be drawn between points.
1	Connect last point specified on preceding card to this one and interpolate into equal parts as specified by I, J data.

Line Segment Terminator Card

Format (I3)

Columns 2-3 = -1 Signals end of line segment cards. Must be included if number of line segment cards is less than number specified on mesh generation card.

= -2 The program was modified to fix the nodal points of each vertical line in the same position, same Z coordinate, as specified on the external boundary line.

Internal Nodal Point Generation

If -2 is specified on the line segment terminator card, the program has been modified to fix the Z coordinate of the internal nodal points to those specified on the external boundary. If this option is

specified, it is only necessary to specify the positions of nodal points on two external boundaries. For example, the boundaries with the Z and R coordinates of zero.

First Card	Format (16I5)
Columns 1-5	IBMAX-the I index of the last column on which nodal points will be fixed.
Columns 6-10	JBMAX-the J index of the last row on which nodal points will be fixed.
Columns 11-15	NUMJ-the number of J indices to be read in on the following card.
Columns 16-20	ICT-I index of the column passing through the center of the crack.
Columns 21-25	JCT-JCT is set equal to ICT.
Columns 26-30	JCMAX-J index of crack tip.

Second Card	Format (16I5) - This card contains the J indices, in sequential order, specified on the boundary with Z coordinate of zero.

A Blank Card Must Appear Here

Shift Axis Card

If coordinate axis are to be moved from the position specified on line segment card, the move can be made with this card. If change is not necessary, leave blank. Format (2F10.0).

Columns 1-10 R shift-shift in R coordinate.

Columns 11-20 Z shift-shift in Z coordinate.

The following data is needed to instruct the program how to perform the transition from course to fine grid.

J Omit Card

Specified the number of J rows which will have segments omitted.

Format (I5) JOMAX

J Segment Cards

Specifies segment of J row that is to be included. Cards must be in sequential order starting from lowest J-index.

Format (3I5)

Columns 1-5	JOMIT	J index of row which segments are to be omitted.
Columns 6-10	MSTART	I index of first nodal point, with J index JOMIT that is to be included.
Columns 11-15	MSTOP	I index of last nodal point, with J index JOMIT that is to be included.

I OMIT Cards

Specifies the number of I columns which will have segments omitted.

Format (I5) IOMAX

I Segment Cards

Specifies segment of the I column which is to be included in the grid pattern. Cards must be in sequential order starting with lowest I index.

Format (3I5)

Columns 1-5	IOMIT	I index of column which segments are to be omitted.
Columns 6-10	LSTART	J index of first nodal point, with I index of IOMIT that is to be included.
Columns 11-15	LSTOP	J index of last nodal point, with I index of IOMIT that is to be included.

Expansion Parameter Card

The information on this card signifies the beginning and the end of the fine gridding in the crack tip region, in terms of the J index.

Format (3I5)

Columns 1-5	IEXPAN	The J index of the row following the last JOMIT index specified in the J segment data.
Columns 6-10	IIEXD	I index of a node point which tells the program that after this point is passed it is to begin generating triangular elements when the nodal points are in the correct formation. This point is directly below the

		crack tip and in the row with a J-index one less than the first JOMIT index specified in the J segment data.
Columns 11-15	JJEXP	J index of the nodal point described in IIEXP.

Material Block Assignment

Each card assigns a material number to a block of elements defined by I-J data. The number of cards must agree with the number specified in columns 11-15 of mesh control data card.

Format (5I5)

Columns 1-5	Material definition number
Columns 6-10	Minimum I
Columns 11-15	Maximum I
Columns 16-20	Minimum J
Columns 21-25	Maximum J

```
C         MAIN PROGRAM
C*************************************************************************
C      SAAS III, FINITE ELEMENT STRESS ANALYSIS OF AXISYMMETRIC AND PLANE
C      SOLIDS WITH DIFFERENT ORTHOTROPIC, TEMPERATURE-DEPENDENT MATERIAL
C      PROPERTIES IN TENSION AND COMPRESSION INCLUDING THE EFFECTS OF
C      INTERNAL PORE FLUID PRESSURES AND THERMAL STRESSES.
C*************************************************************************
       COMMON/BASIC/NUMNP,NUMEL,NUMPC,NUMSC,ACELZ,ANGVEL,TREF,VOL,IFREQ
       COMMON/NPDATA/R(1000),CODE(1000),XR(1000),Z(1000),XZ(1000),T(1000)
       DOUBLE PRECISION CRZ,XI,RR,ZZ,S,RRR,ZZZ
       COMMON/ELDATA/IX(1000,5),EPR(1000),ALPHA(1000),PST(1000)
       COMMON/SOLVE/NCODE(30,100),NUMTC
       COMMON/TD/IMIN(100),IMAX(100),JMIN(30),JMAX(30),MAXI,MAXJ,NMTL,NBC
      1     ,MINI,MINJ
       COMMON /OHG4/ ISTOP
       COMMON/LC2/ KP,RP(250),ZP(250)
       COMMON/JEH/NCHC,IMIV(30),IMAV(30),JMIV(30),JMAV(30)
       COMMON/OHG5/ JSTOP
       INTEGER TITLE(20)
C*************************************************************************
C      READ AND WRITE INPUT DATA CARD IMAGES FOR ALL CASES
C*************************************************************************
       JSTOP=0
  200  CONTINUE
       CALL DATA
        ZFORCE = 0.0
        ELMASS = 0.0
       VOLM=0.0
C*************************************************************************
C      READ AND WRITE CONTROL INFORMATION
C*************************************************************************
       READ(9,1000) TITLE,NPP,ISTART,ISTOP,IDEF,IPLOT,NNLA,IMESH,NUMTC,
      1      NPORPR,NUMMAT,NUMPC,NUMSC,TREF,NTCA,IFREQ
      2    ,IBPLT,NUMNP,NUMEL
       WRITE(6,2000)(TITLE(I),I=1,15),
      1                                  ISTART,ISTOP,IDEF,IPLOT,NNLA,IMESH,
      1      NUMTC,NPORPR,NUMMAT,NUMPC,NUMSC,TREF
      2 ,IBPLT
C*************************************************************************
C      GENERATE FINITE ELEMENT MESH
C*************************************************************************
  215  CALL MESH
C
C      INITIALIZE
C
C*************************************************************************
C      READ AND WRITE NODAL POINT AND ELEMENT DATA
C*************************************************************************
  225 CALL POINTS
C*************************************************************************
C      OUTPUT ELEMENT DATA
C*************************************************************************
       PRINT 3100
       NPRINT=0
       DO 350 N=1,NLMEL
       IF(NPRINT.NE.0)GO TO 300
```

```
      WRITE(6,2008)
      MPRINT=50
  300 MPRINT=MPRINT-1
      NSTRSS=20
      THICK=0.281
  350 WRITE(6,2009) N,(IX(N,I),I=1,5),ALPHA(N),T(N),PST(N),NSTRSS,THICK
      IF( ISTOP .NE. 33 ) GO TO 362
      DO 360 NPUN=1,NUMEL
      PUNCH 3002,NPUN,(IX(NPUN,I),I=1,5),NSTRSS,THICK
  360 CONTINUE
      DO 361 NP=1,NUMNP
      PUNCH 3200,NP,R(NP),Z(NP)
  361 CONTINUE
  362 CONTINUE
  370 IF(ISTOP.EQ.1.OR.ISTOP.EQ.11)GO TO 910
  910 IF( NPP .NE. 0 ) GO TO 200
      IF ( ISTOP .EQ. 1 ) GO TO 200
      IF ( IFREQ .EQ. 0 ) GO TO 200
C     SUM THE ELEMENTS OF THE Z-DIRECTION BOUNDARY FORCE MATRIX
      DO 905 IFOR =1,NUMNP
  905 ZFORCE = ZFORCE + XZ(IFOR)
      ZFORCE = ZFORCE * 2. * 3.1415927
       ELMASS = ELMASS/2.0
       WEIGHT = ELMASS*12.0*32.17
       GFORCE = ELMASS*ACELZ
       ELMASS = ELMASS*12.0
      WRITE (6,3000) ELMASS
      WRITE (6,3001) ZFORCE
       WRITE(6,3003)WEIGHT
       WRITE(6,3004)GFORCE
      GO TO 200
C
1000  FORMAT(20A4,/,
     1            I2,I3,I5,I2,I3,3I5,I3,I2,2I5,F5.0,6I5)
 1001 FORMAT (4F10.0)
2000  FORMAT(1H1,19A4,//,
     1 33H0  START PARAMETER----------------,I4,/
     2 33H0  STOP PARAMETER-----------------,I4,/
     3 33H0  IF 1, PLOT DEFLECTIONS         ,I4,/
     4 32H0  IF 1, SMALL PLOT, IF 2, LARGE,/
     5 33H0  PLOT, OTHERWISE NO PLOT,-------,I4,/
     6 33H0  NUMBER OF APPROXIMATIONS-------,I4,/
     7 33H0  IF 1, GENERATE MESH------------,I4,/
     8 33H0  NUMBER OF TEMPERATURE CARDS----,I4,/
     3 33H0  NUMBER OF MATERIALS------------,I4,/
     4 33H0  NUMBER OF EXTERNAL PRESSURES---,I4,/
     5 33H0  NUMBER OF SHEAR CARDS----------,I4,/
     6 33H0  REFERENCE TEMPERATURE----------,E12.4,/
     7 33H0  BOUNDARY PLOT OPTION           ,I4,//)
 2001 FORMAT (77H A FUNDAMENTAL FREQUENCY WILL BE COMPUTED. A LONGER RUN
     1 TIME WILL BE OBSERVED/80H DUE TO THE NEED TO RECOMPUTE EACH ELEME
     2NT STIFFNESS MATRIX IN SUBROUTINE STRESS)
 2002 FORMAT (24H THE ANGULAR VELOCITY IS,E12.4,/31H AND THE AXIAL ACCEL
     1ERATION IS ,E12.4)
 2003 FORMAT (23H THE R ACCELERATION IS ,E12.4/27H AND THE Z ACCELERATIO
     1N IS ,E12.4)
```

```
 2004 FORMAT (//42H THE PLANE STRAIN OPTION HAS BEEN SELECTED)
 2005 FORMAT (//42H THE PLANE STRESS OPTION HAS BEEN SELECTED)
 2008 FORMAT (88H1  EL    I    J    K    L   MATERIAL    ANGLE    TEMPERATURE
     1     PRESSURE  PRINT      THICKNESS    )
 2009 FORMAT(I5,4I4,I8,F11.1,2F13.3,5X,I5,5X,F10.4)
 2013 FORMAT (30H1 PRESSURE BOUNDARY CONDITIONS)
 2015 FORMAT (27H1 SHEAR BOUNDARY CONDITIONS)
 2020 FORMAT (/29H  THE PROCEDURE CONVERGED IN ,I2,34H TENSION - COMPRES
     1SION ITERATIONS )
 2021 FORMAT (/36H  THE PROCEDURE DID NOT CONVERGE IN ,I2,33H TENSION -
     1COMPRESSION ITERATIONS)
 2022 FORMAT (/29H  THE PROCEDURE CONVERGED IN ,I2,30H NONLINEAR ELASTIC
     1 ITERATIONS )
 2023 FORMAT (/36H  THE PROCEDURE DID NOT CONVERGE IN ,I2,30H NONLINEAR
     1ELASTIC ITERATIONS )
 2030 FORMAT (/51H   NUMBER OF TENSION-COMPRESSION APPROXIMATIONS----,
     1 I4//)
3000  FORMAT(1H ,//,10X, 4HMASS,20(2H..),E20.14,3X,5HSLUGS)
3001  FORMAT(1H ,/,10X,39HAXIAL FORCE DUE TO NORMAL STRESSES,/,10X,
     1                  40HSHEAR STRESSES, AND CONCENTRATED RADIAL, /,
     21H ,10X,          16HAND AXIAL FORCES ,14(2H..), E20.14,3X,3HLBF)
3003  FORMAT(1H ,/,10X, 6HWEIGHT,19(2H..), E20.14,3X, 3HLBF)
3004  FORMAT(1H ,/,10X,20HAXIAL INERTIAL FORCE ,12(2H..),E20.14,3X,
     1 3HLBF)
 3002 FORMAT(6I5,20X,I5,5X,F10.4)
3100  FORMAT(1H ,       12HELEMENT DATA)
 3200 FORMAT(I5,40X,2F10.4)
      END
```

```
C        MESH-- THIS ROUTINE GENERATES THE MESH GIVEN LINE SEGMENT INPUT
      SUBROUTINE MESH
C*************************************************************************
C     NCODE(I,J) = 1  FOR BOUNDARY DEFINITION POINTS
C                = 2  FOR INTERPOLATED BOUNDARY POINTS
C                = 3  FOR INTERPOLATED INTERIOR POINTS
C                = 4  FOR EXTERIOR POINTS
C                = 5  FOR VOID POINTS
C     IPTION = 0  FOR SINGLE POINTS
C            = 1  FOR STRAIGHT LINES
C            = 2  FOR INTERNAL DIAGONAL
C            = 3  FOR 3-POINT ARC
C            = 4  FOR 2 POINT + CENTER ARC
C            = 5  FOR 2 POINT + RADIUS ARC(INITIALIZATION ONLY)
C            = 6  FOR 2 POINT + RADIUS ARC
C*************************************************************************
C
      COMMON/TD/IMIN(100),IMAX(100),JMIN(30),JMAX(30),MAXI,MAXJ,NMTL,NBC
     1    ,MINI,MINJ
      COMMON/NPDATA/R(1000),CODE(1000),AR(1000),Z(1000),AZ(1000),T(1000)
      COMMON/ELDATA/IX(1000,5),EPR(1000),ALPHA(1000),PST(1000)
      COMMON/LC2/ KP,RP(250),ZP(250)
      COMMON/BASIC/NUMNP,NUMEL,NUMPC,NUMSC,ACELZ,ANGVEL,TREF,VOL,IFREQ
      COMMON/OHG4/ISTOP
      COMMON/JEH/NCHC,IMIV(30),IMAV(30),JMIV(30),JMAV(30)
      COMMON/SOLVE/NCODE(30,100),NUMTC
      DIMENSION AR(30,100),AZ(30,100)
      DIMENSION JJB(20)
      EQUIVALENCE(R(1),AR(1,1)),(Z(1),AZ(1,1))
C*************************************************************************
C     MESH CONTROL INFORMATION
C*************************************************************************
      READ (9,1000)NSEG,NBC,NMTL,NLIN,CONI,CONJ,ISET,JSET
      WRITE(6,2000)NSEG,NBC,NMTL,NLIN,CONI,CONJ,ISET,JSET
C*************************************************************************
C     INITIALIZE
C*************************************************************************
      KP=1
      ISEG=0
      PI=3.1415927
      II=1
       IC=0
      DO 110 J=1,100
      DO 100 I=1,30
      NCODE(I,J)=4
      AR(I,J)=0.
  100 AZ(I,J)=0.
      IMIN(J)=30
  110 IMAX(J)=0
      DO 120 I=1,30
      JMAX(I)=0
  120 JMIN(I)=100
C*************************************************************************
C     LINE SEGMENT CARDS
C*************************************************************************
      PRINT 2001
```

```
      READ(9,1001)I2,J2,R2,Z2
      IPTION=1
  130 PRINT 2005
      PRINT 2010,I2,J2,R2,Z2
  200 ISEG=ISEG+1
      I1=I2
      J1=J2
      R1=R2
      Z1=Z2
      AR(I1,J1)=R1
      AZ(I1,J1)=Z1
      RP(KP)=R1
      IF(IPTION.LT.0)RP(KP)=-R1
      ZP(KP)=Z1
      KP=KP+1
      NODE(I1,J1)=1
      CALL MNIMX(I1,J1)
      IF(ISEG.EQ.NSEG) GO TO 500
      IF(IC .EQ. 1 ) GO TO 249
  250 READ(9,1001)I2,J2,R2,Z2,I3,J3,R3,Z3,IPYION
  249 IF(I2.NE. -2.AND.IC.EQ.0) GO TO 251
      IF(I2.NE. -2) GO TO 252
      READ(9,5000) IBMAX,JBMAX,NUMJ,ICT,JCT,JCMAX
 5000 FORMAT(16I5)
      READ(9,5000) (JJB(N),N=1,NUMJ)
      II=II+1
      JJ=1
      I2=II
      J2=JJB(1)
      R2=AR(I2,1)
      Z2=AZ(1,J2)
      IPTION=-1
      I3=0
      J3=0
      R3=0.0
      Z3=0.0
      IC=1
      GO TO 251
  252   IF(I2 .GT. IBMAX ) GO TO 255
      IF(J2.EQ.JBMAX) GO TO 253
      JJ=JJ+1
      I2=II
      J2=JJB(JJ)
      IF(I2.GE.ICT.AND.I2.LE.JCT.AND.J2.GT.JCMAX) GO TO 253
      IPTION=1
      GO TO 254
  253 II=II+1
      JJ=1
       I2=II
      IF(I2.GT. IBMAX) GO TO 255
      J2=JJB(1)
       IPTION=-1
  254 R2=AR(I2,1)
      Z2=AZ(1,J2)
      IC=1
      GO TO 251
```

```
  255  IC=0
       I2=-1
       GO TO 251
  251  IF(I2 .EQ. -1 ) GO TO 500
       IF(IPTION.LT.0)GO TO 130
       WRITE(6,2010)I2,J2,R2,Z2,I3,J3,R3,Z3,IPTION
       IPTION=IPTION+1
       GO TO ( 200,300,300,346,346,346,346) , IPTION
C*************************************************************************
C      GENERATE STRAIGHT LINES ON BOUNDARY
C*************************************************************************
  300  DI=ABS(FLOAT(I2-I1))
       DJ=ABS(FLOAT(J2-J1))
       ISTRT=I1
       ISTP=I2
       JSTRT=J1
       JSTP=J2
       DIFF=AMAX1(DI,DJ)
       ITER=DIFF-1.
       IINC=0
       JINC=0
       IF(I2.NE.I1) IINC=(I2-I1)/IABS(I2-I1)
       IF(J2.NE.J1) JINC=(J2-J1)/IABS(J2-J1)
       KAPPA=1
       IF(I2.NE.I1.AND.J2.NE.J1.AND.IPTION.NE.3) KAPPA=2
       IF(KAPPA.EQ.2) DIFF=2.*DIFF
       RINC=(R2-R1)/DIFF
       ZINC=(Z2-Z1)/DIFF
       WRITE(6,2002) DI,DJ,DIFF,RINC,ZINC,ITER,IINC,JINC,KAPPA
C
C      CHECK FOR INPUT ERROR
C
       IF(IPTION.EQ.3 .AND.DI.NE.DJ) GO TO 310
       IF(KAPPA.NE.2.OR.DI.EQ.DJ) GO TO 320
  310  WRITE(6,2003)
       GO TO 200
C
C      INTERPOLATE
C
  320  I=I1
       J=J1
       WRITE(6,2004)
       WRITE(6,2004)
       DO 340 M=1,ITER
       IF(ITER.EQ.0.AND.IPTION.EQ.2)GO TO 345
       IF(KAPPA.EQ.2) GO TO 330
       IOLD=I
       I=I+IINC
       JOLD=J
       J=J+JINC
       AR(I,J)=AR(IOLD,JOLD)+RINC
       AZ(I,J)=AZ(IOLD,JOLD)+ZINC
       WRITE(6,2005) I,J,AR(I,J),AZ(I,J)
       CALL MNIMX(I,J)
       IF(NCODE(I,J).NE.4)WRITE(6,2100)I,J
       NCODE(I,J)=2
```

```
      GO TO 340
  330 IOLD=I
      I=I+IINC
      AR(I,J)=AR(IOLD,J)+RINC
      AZ(I,J)=AZ(IOLD,J)+ZINC
      WRITE(6,2005) I,J,AR(I,J),AZ(I,J)
      IF(NCODE(I,J).NE.4)WRITE(6,2100)I,J
      NODE(I,J)=2
      CALL MNIMX(I,J)
      JOLD=J
      J=J+JINC
      AR(I,J)=AR(I,JOLD)+RINC
      AZ(I,J)=AZ(I,JOLD)+ZINC
      IF(NCODE(I,J).NE.4)WRITE(6,2100)I,J
      NODE(I,J)=2
      WRITE(6,2005) I,J,AR(I,J),AZ(I,J)
      CALL MNIMX(I,J)
  340 CONTINUE
  345 IF(KAPPA.EQ.1) GO TO 200
      IOLD=I
      I=I+IINC
      AR(I,J)=AR(IOLD,J)+RINC
      AZ(I,J)=AZ(IOLD,J)+ZINC
      IF(NCODE(I,J).NE.4)WRITE(6,2100)I,J
      NODE(I,J)=2
      WRITE(6,2005) I,J,AR(I,J),AZ(I,J)
      CALL MNIMX(I,J)
      GO TO 200
  346 WRITE(6,4001)
 4001 FORMAT('0','***** INPUT ERROR ----VALUE OF IPTION GREATER THEN 1
     :-----EXECUTION TERMINATED')
      STOP
C*****************************************************************************
  500 MAXI=0
      MAXJ=0
      MINI=30
      MINJ=100
      DO 503 I=1,30
      IF(JMAX(I).GT.MAXJ)MAXJ=JMAX(I)
      IF(JMIN(I).LT.MINJ)MINJ=JMIN(I)
  503 CONTINUE
      DO 507 J=1,100
      IF(IMAX(J).GT.MAXI)MAXI=IMAX(J)
      IF(IMIN(J).LT.MINI)MINI=IMIN(J)
  507 CONTINUE
      READ (9,1000)NOHC
      IF(NOHC.EQ.0)GO TO 511
      WRITE(6,8500)
      DO 508 NO=1,NOHC
      READ (9,8000)IMI,IMA,JMI,JMA
      WRITE(6,8000)IMI,IMA,JMI,JMA
      IMIV(NO)=IMI
      IMAV(NO)=IMA
      JMIV(NO)=JMI
      JMAV(NO)=JMA
      DO 508 J=JMI,JMA
```

```
      DO 508 I=IMI,IMA
  508 NOCDE(I,J)=5
 8000 FORMAT(4I5)
 8500  FORMAT(1H0, 20HVOID SPECIFICATIONS ,/,
     1           21H   IMI   IMA   JMI   JMA )
      IF(NOHC.LE.30)GO TO 511
      WRITE(6,9000)
 9000 FORMAT(33H0****ERROR****TOO MANY VOID CARDS)
      STOP
C*************************************************************************
C     CALCULATE COORDINATES OF INTERIOR POINTS
C*************************************************************************
  511 IF ( MAXI+1 .LE. 2 ) GO TO 530
      I1=MINI+1
      I2=MAXI-1
      IF(NLIM.LT.1) NLIM = 100
      DO 520 N=1,NLIM
      RESID=0.
      DO 510 I=I1,I2
      J1=JMIN(I)+1
      J2=JMAX(I)-1
      DO 510 J=J1,J2
      KODE=NCODE(I,J)
      GO TO(510,510,509,506,510),KODE
  506 NOCDE(I,J)=3
  509 DR=(AR(I+1,J)+AR(I-1,J)+AR(I,J+1)+AR(I,J-1))/4.-AR(I,J)
     1 +CONI * (AR(I+1,J) - AR(I-1,J))/FLOAT(8*(I+ISET))
     2 + CONJ * (AR(I,J+1) - AR(I,J-1)) / FLOAT(8*(J+JSET))
      DZ=(AZ(I+1,J)+AZ(I-1,J)+AZ(I,J+1)+AZ(I,J-1))/4.-AZ(I,J)
     1 + CONJ * (AZ(I,J+1) - AZ(I,J-1))/FLOAT(8*(J+JSET))
     2 + CONI * (AZ(I+1,J) - AZ(I-1,J)) / FLOAT(8*(I+ISET))
      RESID=RESID+ABS(DR)+ABS(DZ)
      AR(I,J)=AR(I,J)+1.8*DR
      AZ(I,J)=AZ(I,J)+1.8*DZ
  510 CONTINUE
      IF(N.EQ.1) RES1=RESID
      IF(N.EQ.1.AND.RESID.EQ.0) GO TO 530
      IF(RESID/RES1.LT.1.E-4) GO TO 530
  520 CONTINUE
  530 WRITE(6,2009) N
      KP=KP-1
  600 CONTINUE
  999 WRITE(6,4000)
 4000  FORMAT(1H ,  9HEND MESH )
C*************************************************************************
C*************************************************************************
C
 1000 FORMAT(4I5,       2F10.0,3I5)
 1001 FORMAT (2(2I3,2F8.3),I5)
 2000 FORMAT (30H1  MESH GENERATION INFORMATION//
     3 41H0  NUMBER OF LINE SEGMENT CARDS----------,I3,/
     4 41H0  NUMBER OF BOUNDARY CONDITION CARDS----,I3,/
     5 41H0  NUMBER OF MATERIAL BLOCK CARDS--------,I3,/
     4 41H0  NUMBER OF BOUNDARY CONDITION CARDS----,I3,/
     5 41H0  NUMBER OF MATERIAL BLOCK CARDS--------,I3,/
     6 41H0  NUMBER OF ITERATIONS------------------,I3,/
```

```
     7 41H0  POLAR COORDINATE PARAMETER I----------,E12.4,/
     8 41H0  POLAR COORDINATE PARAMETER J----------,E12.4,/
     9 41H0  I CURVATURE MODIFICATION-------------,I3,/
     1 41H0  J CURVATURE MODIFICATION-------------,I3,///)
2001  FORMAT(1H0, 81H  INPUT    I   J     R        Z     I2  J2    R2
     1 Z                        IPTION )
2002  FORMAT(1H ,  5H  DI=,F4.0,  5H  DJ=,F4.0,  7H  DIFF=,F4.0,
     1             7H  RINC=,F8.3,     7H  ZINC=,F8.3,7H  ITER=,I3,
     2             7H  IINC=,I3,       7H  JINC=,I3,  8H  KAPPA=,I2)
 2003 FORMAT (1X,38H**BAD INPUT--THIS LINE IS NOT DIAGONAL)
 2004 FORMAT (30H    I    J         AR         AZ)
 2005 FORMAT (2I5,2F10.3)
 2006 FORMAT (51H ** BAD INPUT - THESE POINTS DO NOT DEFINE A CIRCLE,/,
     13X,6F12.4,10X,2E20.8)
2007  FORMAT(1H , 21H  CENTER COORDINATE (,F8.3,1H,,F8.3,1H))
2008  FORMAT(1H ,  7H  ANG1=,F9.6,7H  ANG2=,F9.6,7H  DIFF=,F3.0,
     1   9H  DELPHI=,F9.6)
2009  FORMAT(1H0, 30H  COORDINATES CALCULATED AFTER ,I3,
     1            11H ITERATIONS )
 2010 FORMAT(7X,2(2I4,2F8.3),I6)
 2100 FORMAT(54H*****WARNING***** NODAL POINT WITH (I,J) COORDINATES (,
     1  I2,1H,,I2,21H) HAS BEEN RE-DEFINED)
 3000 FORMAT(16I5)
 3100 FORMAT(2E15.8,I10)
 3200 FORMAT(8F10.5)
      RETURN
      END
```

```
C        POINTS-- THIS RCUTINE ASSIGNS MATERIALS, TEMPERATURES, ETC.
      SUBROUTINE PCINTS
C
      COMMON/BASIC/NUMNP,NUMEL,NUMPC,NUMSC,ACELZ,ANGVEL,TREF,VOL,IFREQ
      COMMON/NPDATA/R(1000),CODE(1000),XR(1000),Z(1000),XZ(1000),T(1000)
      COMMON/ELDATA/IX(1000,5),EPR(1000),ALPHA(1000),PST(1000)
      DOUBLE PRECISION X,Y,TEM
      COMMON/SOLVE/NCODE(30,100),NUMTC
      COMMON/TD/IMIN(100),IMAX(100),JMIN(30),JMAX(30),MAXI,MAXJ,NMTL,NBC
     1    ,MINI,MINJ
      COMMON/PLANE/NPP
      COMMON/JEH/NCHC,IMIV(30),IMAV(30),JMIV(30),JMAV(30)
      COMMON/OHG4/ ISTOP
      DIMENSION AR(30,100),AZ(30,100),MATRIL(20,5),BLKANG(20)
      DIMENSION IORDER(30,100)
      DIMENSION JOMIT(40),MSTART(40),MSTOP(40)
      DIMENSION IOMIT(40),LSTART(40),LSTOP(40)
      DATA IORDER/3000*0/
      EQUIVALENCE (R(1),AR(1,1)),(Z(1),AZ(1,1))
C*************************************************************************
      READ(9,4999) RSHIF,ZSHIF
 4999 FORMAT(2F10.0)
      READ(9,5000) JOMAX
 5000 FORMAT(I5)
      DO 7 J0=1,JOMAX
      READ(9,5001) JOMIT(J0),MSTART(J0),MSTOP(J0)
 5001 FORMAT(3I5)
 7    CONTINUE
      READ(9,5004) IOMAX
 5004 FORMAT(I5)
      DO 6 I0=1,IOMAX
 6    READ(9,5001) IOMIT(I0),LSTART(I0),LSTOP(I0)
      READ(9,5001) IEXPAN,IIEXP,JJEXP
      NP=0
      J0=1
      DO 120 J=MINJ,MAXJ
      IF( J .EQ. JOMIT(J0) ) GO TO 90
      NSTART=IMIN(J)
      NSTOP=IMAX(J)
      GO TO 91
 90   NSTART=MSTART(J0)
      NSTOP=MSTOP(J0)
      J0=J0+1
 91   I0=1
      DO 120 I=NSTART,NSTOP
      IORDER(I,J)=0
      IF(NCODE(I,J).EQ.4) GO TO 120
      IF(I.NE.IOMIT(I0)) GO TO 96
      IF(J.LE.LSTOP(I0) ) GO TO 92
      GO TO 93
 92   IF(J .GE. LSTART(I0) ) GO TO 95
 93   I0=I0+1
      GO TO 120
 95   I0=I0+1
 96   NP=NP+1
      R(NP)=AR(I,J)
```

```
      Z(NP)=AZ(I,J)
      IORDER(I,J)=NP
  120 CONTINUE
      NUMNP=NP
C*****************************************************************************
C     READ AND ASSIGN BOUNDARY CONDITIONS
C*****************************************************************************
C     INITIALIZE
C
      DO 150 I=1,1000
      T(I)=0.0
  150 PSY(I)=0.0
      DO 200 I=1,NUMNP
      CODE(I)=0.
      IF(R(I).EQ.0..AND.NPP.EQ.0) CODE(I) = 1.
      XR(I)=0.
      XZ(I)=0.
  200 CONTINUE
C
      IF(NBC.EQ.0) GO TO 220
      DO 210 IBCON=1,NBC
      READ(9,1002) I1,I2,J1,J2,CON,RCON,ZCON
      DO 210 I=I1,I2
      DO 210 J=J1,J2
      NP=IORDER(I,J)
      CODE(NP)=CON
      XR(NP)=RCON
  210 XZ(NP)=ZCON
  220 MPRINT=0
      PRINT 1300,NUMNP
      NP=0
      J0=1
      DO 240 J=MIN0,MAXJ
      IF( J .EQ. JOMIT(J0) ) GO TO 225
      NSTART=IMIN(J)
      NSTOP=IMAX(J)
      GO TO 226
  225 NSTART=MSTART(J0)
      NSTOP=MSTOP(J0)
      J0=J0+1
  226 I0=1
      DO 240 I=NSTART,NSTOP
      IF ( NCODE(I,J) .EQ. 4 ) GO TO 240
      IF(I.NE.IOMIT(I0) ) GO TO 256
      IF(J .LE.LSTOP(I0) ) GO TO 254
      GO TO 257
  254 IF(J .GE. LSTART(I0) ) GO TO 255
  257 I0=I0+1
      GO TO 240
  255 I0=I0+1
  256 NP=NP+1
      IF(MPRINT.NE.0) GO TO 230
      WRITE(6,2000)
      MPRINT=50
  230 MPRINT=MPRINT-1
      R(NP)=R(NP)-RSHIF
```

```
      Z(NP)=Z(NP)-ZSHIF
      WRITE(6,2001)I,J,NP,CODE(NP),R(NP),Z(NP),XR(NP),XZ(NP),NCODE(I,J)
  240 CONTINUE
C*****************************************************************************
C     ASSIGN MATERIALS IN BLOCKS
C*****************************************************************************
      DO 300 M1=1,1000
  300 IX(M1,5)=0
      DO 310 IMTL=1,NMTL
      READ (9,1000) MTL,(MATRIL(IMTL,IM),IM=2,5),BLKANG(MTL)
  310 MATRIL(IMTL,1)=MTL
C*****************************************************************************
C     ESTABLISH ELEMENT INFORMATION
C*****************************************************************************
      JJMAX=MAXJ-1
      IOCODE=1
      JOCODE=1
      JJCODE=1
      NEL=0
      JJ=0
      II=0
      GO TO 312
  311 CONTINUE
  312 JJ=JJ+1
      IF(JJ .GT. JJMAX) GO TO 400
      JJCODE=1
      II=0
      NSTART=IMIN0(JJ)
      NSTOP=IMAX(JJ)
      II=NSTART
       GO TO 314
  313 II=II+1
      IF(II.GE.NSTOP) GO TO 311
  314 IF(IORDER(II,JJ) .EQ. 0 ) GO TO 313
      IIP=II+1
      JJP=JJ+1
      IF ( NCODE(II,JJ) .EQ. 4 ) GO TO 317
      IF(NCODE(IIP,JJ ).EQ.4)GO TO 317
      IF(NCODE(II ,JJP).EQ.4)GO TO 317
      IF(NCODE(IIP,JJP).EQ.4)GO TO 317
      IF(JJ.GE.JJEXP.AND.II.GE.IIEXP) GO TO 316
      IF(NCODE(II ,JJ ).NE.5)GO TO 318
      IF(NCODE(IIP,JJ ).NE.5)GO TO 318
      IF(NCODE(II ,JJP).NE.5)GO TO 318
      IF(NCODE(IIP,JJP).NE.5)GO TO 318
      DO 315 NO=1,NOMC
      IF(II.GE.IMIV(NO).AND.II.LE.IMAV(NO).AND.
     1   JJ.GE.JMIV(NO).AND.JJ.LE.JMAV(NO).AND.
     2   IIP.GE.IMIV(NO).AND.IIP.LE.IMAV(NO).AND.JJP.GE.JMIV(NO).AND.
     3   JJP.LE.JMAV(NO))GO TO 313
  315 CONTINUE
  316 JJCODE=2
      GO TO 318
  317 JJCODE=2
      GO TO 313
  318 CONTINUE
```

```
C     CHECK FOR  DIRECTION OF EXPANSION
      IF(JJCODE.EQ.2) GO TO 320
 319  CONTINUE
      IF(IORDER(II,JJ).GT.0.AND.IORDER(II,JJP).GT.0)GO TO 333
      IF(IORDER(II,JJ).GT.0.AND.IORDER(IIP,JJ).GT.0) GO TO 321
      WRITE(6,6000) II,JJ,IIP,JJP
 6000 FORMAT(' ',' ***ERROR***  POINTS',4I5,'  DO NOT DEFINE A VALID
     * EXPANSION EXECUTION TERMINATED')
      STOP
 320  CONTINUE
      IF( JJ .GE. IEXPAN ) GO TO 319
      IF(IORDER(IIP,JJ) .EQ. 0 ) GO TO 313
      IF(IORDER(IIP,JJP).EQ.0) GO TO 321
      GO TO 319
 321  CONTINUE
C     EXPANSION IN J-DIRECTION
      IF(IORDER(II,JJP).EQ.0.AND.IORDER(IIP,JJP).EQ.0) GO TO 331
      IF(IORDER(II,JJP).GT.0.AND.IORDER(IIP,JJP).GT.0) GO TO 329
      IF(IORDER(II,JJP).EQ.0) GO TO 322
      IITEMP=II
      JJTEMP=JJP
      JCODE=3
      GO TO 331
 322  IITEMP=IIP
      JJTEMP=JJP
      JCODE=2
      GO TO 331
 323  CONTINUE
C     TRIANGULAR ELEMENTS
      IA=IORDER(II,JJ)
      IB=IORDER(IIP,JJ)
      IC=IORDER(IITEMP,JJTEMP)
      ID=IC
      GO TO 332
 324  IA=IORDER(II,JJ)
      IB=IORDER(IITEMP,JJTEMP)
      IC=IORDER(II,JJP)
      ID=IC
      JCODE=4
      GO TO 332
 325  IA=IORDER(II,JJP)
      IB=IORDER(IITEMP,JJTEMP)
      IC=IORDER(IIP,JJP)
      ID=IC
      JCODE=1
      GO TO 332
 326  IA=IORDER(II,JJ)
      IB=IORDER(IIP,JJ)
      IC=IORDER(IITEMP,JJTEMP)
      ID=IC
      GO TO 332
 327  IA=IORDER(IIP,JJ)
      IB=IORDER(IIP,JJP)
      IC=IORDER(IITEMP,JJTEMP)
      ID=IC
      JCODE=5
```

```
      GO TO 332
  328 IA=IORDER(IIP,JJP)
      IB=IORDER(II,JJP)
      IC=IORDER(IITEMP,JJTEMP)
      ID=IC
      JCODE=1
      GO TO 332
  329 GO TO (330,323,326) ,JCODE
  330 IA=IORDER(II,JJ)
      IB=IORDER(IIP,JJ)
      IC=IORDER(IIP,JJP)
      ID=IORDER(II,JJP)
      GO TO 332
  331 JJP=JJP+1
      IF(JJP.GT.MAXJ) CALL ERROR(1,JJP,MAXJ,II)
      GO TO 321
  332 NEL=NEL+1
      IF(NEL.GT.1000) CALL ERROR(2,NEL,1000,0)
      IX(NEL,1)=IA
      IX(NEL,2)=IB
      IX(NEL,3)=IC
      IX(NEL,4)=ID
      IX(NEL,5)=MTL
      ALPHA(NEL)=BLKANG(MTL)
      GO TO ( 345,324,327,325,328 ),JCODE
  333 CONTINUE
C     EXPANSION IN I-DIRECTION
      IF(IORDER(IIP,JJ).EQ.0.AND.IORDER(IIP,JJP).EQ.0) GO TO 337
      IF(IORDER(IIP,JJ).GT.0.AND.IORDER(IIP,JJP).GT.0) GO TO 335
      IF(IORDER(IIP,JJ).EQ.0) GO TO 334
      IITEMP=IIP
      JJTEMP=JJ
      ICODE=2
      GO TO 337
  334 IITEMP=IIP
      JJTEMP=JJP
      ICODE=3
      GO TO 337
  335 GO TO (336,342,339) ,ICODE
  336 IA=IORDER(II,JJ)
      IB=IORDER(IIP,JJ)
      IC=IORDER(IIP,JJP)
      ID=IORDER(II,JJP)
      II=IIP-1
      GO TO 338
  337 IIP=IIP+1
      IF(IIP.GT.NSTOP) CALL ERROR(3,IIP,NSTOP,JJ)
      GO TO 333
  338 NEL=NEL+1
      IF(NEL.GT.1000) CALL ERROR(2,NEL,1000,0)
      IX(NEL,1)=IA
      IX(NEL,2)=IB
      IX(NEL,3)=IC
      IX(NEL,4)=ID
      IX(NEL,5)=MTL
      ALPHA(NEL)=BLKANG(MTL)
```

```
      GO TO ( 345,343,340,341,344 ), ICODE
  339 CONTINUE
C     TRIANGULAR ELEMENTS
      IA=IORDER(II,JJ)
      IB=IORDER(IITEMP,JJTEMP)
      IC=IORDER(II,JJP)
      ID=IC
      GO TO 338
  340 IA=IORDER(II,JJ)
      IB=IORDER(IIP,JJ)
      IC=IORDER(IITEMP,JJTEMP)
      ID=IC
      IOCDE=4
      GO TO 338
  341 IA=IORDER(IIP,JJ)
      IB=IORDER(IIP,JJP)
      IC=IORDER(IITEMP,JJTEMP)
      ID=IC
      II=IIP-1
      IOCDE=1
      GO TO 338
  342 IA=IORDER(II,JJ)
      IB=IORDER(IITEMP,JJTEMP)
      IC=IORDER(II,JJP)
      ID=IC
      GO TO 338
  343 IA=IORDER(II,JJP)
      IB=IORDER(IITEMP,JJTEMP)
      IC=IORDER(IIP,JJP)
      ID=IC
      IOCDE=5
      GO TO 338
  344 IA=IORDER(IIP,JJ)
      IB=IORDER(IIP,JJP)
      IC=IORDER(IITEMP,JJTEMP)
      ID=IC
      II=IIP-1
      IOCDE=1
      GO TO 338
  345 DO 360 IMTL=1,NMTL
      IF(II.LT.MATRIL(IMTL,2))GO TO 360
      IF(II.GE.MATRIL(IMTL,3))GO TO 360
      IF(JJ.LT.MATRIL(IMTL,4))GO TO 360
      IF(JJ.GE.MATRIL(IMTL,5))GO TO 360
      MTL = MATRIL(IMTL,1)
      GO TO 380
  360 CONTINUE
      PRINT 2100,NEL,II,JJ
      MTL=1
  380 IX(NEL,5)=MTL
      ALPHA(NEL)=BLKANG(MTL)
      GO TO 313
  400 CONTINUE
      NUMEL=NEL
  480 IF(NUMNP.GT.1000) WRITE(6,2002)
C*****************************************************************
```

```
C      SET NODAL POINT TEMPERATURE TO REFERENCE TEMPERATURE
C*************************************************************************
       IF(NUMTC.NE.0)GO TC 550
       DO 500 N=1,NUMNP
  500  T(N)=TREF
  550  WRITE(6,4000)
4000   FORMAT(1H , 10HEND POINTS )
       RETURN
C
 1000  FORMAT (5I5,F10.0)
 1002  FORMAT (4I5,3F10.0)
1300   FORMAT(1H0, 40HNODAL POINT DATA---NO. OF NODAL POINTS= ,I5)
 2000  FORMAT( 104H1    I     J     NP         TYPE     R-ORDINATE     Z-ORDINA
     1TE   R LOAD OR DISPLACEMENT  Z LOAD OR DISPLACEMENT)
 2001  FORMAT(2I5,I6,F12.1,F12.3,F14.3,E26.7,E24.7,I15)
 2002  FORMAT (35H  BAD INPUT - TOO MANY NODAL POINTS)
2100   FORMAT(1H0, 8HELEMENT ,I4,3X,23HWITH (I,J) COORDINATES(,I2,1H,,I3,
      1             31H) HAS BEEN ASSIGNED MATERIAL 1 )
       END
```

```
C       DATA--- THIS ROUTINE READS CARDS AND PUTS THEM ON TAPE NO.9
      SUBROUTINE DATA
      COMMON/OMG5/ JSTOP
      DIMENSION CARD(20)
      REWIND 9
      N=0
      IF ( JSTOP .EQ. 1 ) GO TO 400
      READ(5,1000) CARD
   10 WRITE(6,1002)
      GO TO 200
100   READ(5,1000,END=300)CARD
  200 WRITE(6,1003)CARD
      WRITE(9,1000) CARD
      N=N+1
      GO TO 100
  300 ENDFILE 9
      REWIND 9
      WRITE(6,1004)
      JSTOP=1
      RETURN
  400 WRITE(6,1005)
      STOP
1000  FORMAT(20A4)
 1002 FORMAT(1H1              /13X,2H10,8X,2H20,8X,2H30,8X,2H40,8X,2H50,
     18X,2H60,8X,2H70,8X,2H80/5X,80H12345678901234567890123456789012345
     278901234567890123456789012345678901234567890)
1003  FORMAT(5X,20A4)
1004  FORMAT(1H , 11HEND OF DATA)
1005  FORMAT(1H , 10HEND OF JOB)
      END
```

```
C        MNINX-- THIS IS A UTILITY ROUTINE
      SUBROUTINE MNIMX(I,J)
C
      COMMON/TD/IMIN(100),IMAX(100),JMIN(30),JMAX(30),MAXI,MAXJ,NMTL,NBC
     1    ,MINI,MINJ
C
      IF(J.LT.JMIN(I)) JMIN(I)=J
      IF(J.GT.JMAX(I)) JMAX(I)=J
      IF(I.LT.IMIN(J)) IMIN(J)=I
      IF(I.GT.IMAX(J)) IMAX(J)=I
C
      RETURN
      END
```

```
C        NODE-- A SMALL UTILITY ROUTINE WHICH MAY BE NEEDED BY MESH OR POINTS
      FUNCTION NODE(I,J)
C
      COMMON/TD/IMIN(100),IMAX(100),JMIN(30),JMAX(30),MAXI,MAXJ,NMTL,NBC
     1    ,MINI,MINJ
C
      NODE=0
      DO 100 JJ=1,J
      NSTART=IMIN(JJ)
      NSTOP=IMAX(JJ)
      DO 100 II=NSTART,NSTOP
      NODE=NODE+1
      IF(JJ.EQ.J.AND.II.EQ.I) RETURN
  100 CONTINUE
C
      RETURN
      END
```

```
      SUBROUTINE ERROR(N,M,L,K)
      GO TO (1,2,3),N
1     WRITE(6,10) M,L,K
10    FORMAT(' ',' JJP= ',I5,'EXCEEDS JJMAX = ',I5,'II= ',I5)
      GO TO 50
2     WRITE(6,11) M,L
11    FORMAT(' ',' NEL = ',I5,'EXCEEDS MAXNEL = ',I5)
      GO TO 50
3     WRITE(6,12) M,L,K
12    FORMAT(' ',' IIP = ',I5,'EXCEEDS NSTOP = ',I5,'JJ = ',I5)
50    WRITE(6,13)
13    FORMAT(' ',' EXECUTION TERMINATED')
      STOP
      END
```

DISTRIBUTION

Commander (NSEA 09G32)
Naval Sea Systems Command
Department of the Navy
Washington, DC 20362 — Copies 1 and 2

Commander (NSEA 0342)
Naval Sea Systems Command
Department of the Navy
Washington, DC 20362 — Copies 3 and 4

Defense Documentation Center
5010 Duke Street
Cameron Station
Alexandria, VA 22314 — Copies 5 through 16

Via: Commander (NSEA 09G32)
Naval Sea Systems Command
Department of the Navy
Washington, DC 20362